Takekida, K., Kikuchi, Y., Yamazaki, T. & 7 other authors (2002). Quantitative analysis of prion protein by immunoblotting. *J Health Sci* **48**, 288–291.

Taraboulos, A., Serban, D. & Prusiner, S. B. (1990). Scrapie prion proteins accumulate in the cytoplasm of persistently infected cultured cells. *J Cell Biol* **110**, 2117–2132.

van Keulen, L. J., Schreuder, B. E., Meloen, R. H., Poelen-van den Berg, M., Mooij-Harkes, G., Vromans, M. E. & Langeveld, J. P. (1995). Immunohistochemical detection and localization of prion protein in brain tissue of sheep with natural scrapie. *Vet Pathol* **32**, 299–308.

Vey, M., Pilkuhn, S., Wille, H., Nixon, R., DeArmond, S. J., Smart, E. J., Anderson, R. G. W., Taraboulos, A. & Prusiner, S. B. (1996). Subcellular colocalization of the cellular and scrapie prion proteins in caveolae-like membranous domains. *Proc Natl Acad Sci U S A* **93**, 14945–14949.

Yedidia, Y., Horonchik, L., Tzaban, S., Yanai, A. & Taraboulos, A. (2001). Proteasomes and ubiquitin are involved in the turnover of the wild-type prion protein. *EMBO J* **20**, 5383–5391.

Journal of General Virology (2004), 85, 3473–3482 DOI 10.1099/vir.0.80113-0

Cell-surface retention of PrP^C by anti-PrP antibody prevents protease-resistant PrP formation

Chan-Lan Kim,[1] Ayako Karino,[1] Naotaka Ishiguro,[1] Morikazu Shinagawa,[1]† Motoyoshi Sato[2] and Motohiro Horiuchi[1]‡

Correspondence
Motohiro Horiuchi
horiuchi@vetmed.hokudai.ac.jp

Laboratory of Veterinary Public Health[1] and Laboratory of Veterinary Radiology[2], Obihiro University of Agriculture and Veterinary Medicine, Inada-cho, Obihiro, Hokkaido 080-8555, Japan

The C-terminal portion of the prion protein (PrP), corresponding to a protease-resistant core fragment of the abnormal isoform of the prion protein (PrP^{Sc}), is essential for prion propagation. Antibodies to the C-terminal portion of PrP are known to inhibit PrP^{Sc} accumulation in cells persistently infected with prions. Here it was shown that, in addition to monoclonal antibodies (mAbs) to the C-terminal portion of PrP, a mAb recognizing the octapeptide repeat region in the N-terminal part of PrP that is dispensable for PrP^{Sc} formation reduced PrP^{Sc} accumulation in cells persistently infected with prions. The 50 % effective dose was as low as ~1 nM, and, regardless of their epitope specificity, the inhibitory mAbs shared the ability to bind cellular prion protein (PrP^C) expressed on the cell surface. Flow cytometric analysis revealed that mAbs that bound to the cell surface during cell culture were not internalized even after their withdrawal from the growth medium. Retention of the mAb–PrP^C complex on the cell surface was also confirmed by the fact that internalization was enhanced by treatment of cells with dextran sulfate. These results suggested that anti-PrP mAb antagonizes PrP^{Sc} formation by interfering with the regular PrP^C degradation pathway.

Received 16 March 2004
Accepted 26 July 2004

INTRODUCTION

Transmissible spongiform encephalopathies (TSEs), also called prion diseases, are fatal neurodegenerative diseases and include scrapie in sheep and goats, bovine spongiform encephalopathy and Creutzfeldt–Jakob disease (CJD) in humans. The causative agent of TSEs, often called a prion, is composed mainly of an abnormal isoform (PrP^{Sc}) of the host cellular prion protein (PrP^C). Mice with genetic knockout of the PrP gene are resistant to prion disease (Bueler *et al.*, 1993) and neurons lacking PrP^C expression are resistant to degeneration, regardless of the presence of PrP^{Sc} (Mallucci *et al.*, 2003). Thus, PrP^C is essential for prion propagation and pathogenesis.

Conversion of PrP^C to PrP^{Sc} is believed to involve direct interaction of the two PrP isoforms. Although the molecular mechanism of conversion is not yet fully understood, it is known that mature PrP^C expressed on the cell surface is a substrate for PrP^{Sc} formation, and a process that involves a conformational transformation takes place in subcellular compartments associated with the degradation pathway of PrP^C, including a sphingolipid-rich membrane microdomain, called a lipid raft (Caughey & Raymond, 1991; Naslavsky *et al.*, 1997; Vey *et al.*, 1996).

Because of the emergence of variant CJD and iatrogenic CJD by dura matter transplantation, especially in Japan, the establishment of therapeutics for prion disease is urgently needed. Therapeutics have been directed at the binding of the two PrP isoforms, as well as the process of conformational transformation, since the conversion of PrP^C to PrP^{Sc} is associated with neuronal pathogenicity. To date, many substances have been reported to inhibit PrP^{Sc} formation in cell culture and/or cell-free systems, including amyloid-binding dyes (Caughey & Race, 1992), sulfated glycosaminoglycans (Caughey & Raymond, 1993), tetrapyrrole compounds (Caughey *et al.*, 1998), cysteine protease inhibitors (Doh-Ura *et al.*, 2000), substituted tricyclic derivatives such as chlorpromazine and quinacrine (Doh-Ura *et al.*, 2000; Korth *et al.*, 2001), branched polyamines (Supattapone *et al.*, 1999, 2001), peptides (Chabry *et al.*, 1998; Soto *et al.*, 2000) and conversion-incompetent PrP (Holscher *et al.*, 1998; Horiuchi *et al.*, 2000; Kaneko *et al.*, 1997). Some of these have already been examined *in vivo*. For instance, sulfated glycosaminoglycans and tetrapyrrole compounds were effective when administered at early stages of infection or simultaneously with the scrapie-affected brain inoculum (Ehlers & Diringer, 1984; Ladogana

†Present address: Prion Disease Research Center, National Institute of Animal Health, Kannondai, Tsukuba, Ibaragi, 305-0856, Japan.

‡Present address: Laboratory of Prion Diseases, Graduate School of Veterinary Medicine, Hokkaido University, Kita 18, Nishi 9, Kita-ku, Sapporo 060-0818, Japan.

et al., 1992; Priola *et al.*, 2000). Polyene antibiotics prolonged the incubation period, even when administered at the middle-late stage of infection (Demaimay *et al.*, 1997), but the effects appeared to depend on the prion strains and host animals studied (Demaimay *et al.*, 1999; Xi *et al.*, 1992). Recently, Doh-Ura and colleagues (2004) showed that intraventricular administration of pentosan polysulfate and quinine prolonged the incubation periods in a prion-infected transgenic mouse model, even at a late stage of infection (Doh-Ura *et al.*, 2004; Murakami-Kubo *et al.*, 2004). Further *in vivo* studies are expected to lead to the establishment of effective therapeutics for prion diseases. However, to achieve more efficient therapeutics, it is essential to elucidate the mechanisms of action and to investigate proper delivery of drugs based on pharmacokinetics.

Anti-PrP antibodies have also been reported to inhibit the formation of PrP^{Sc} in cultured cells and/or cell-free systems (Enari *et al.*, 2001; Horiuchi & Caughey, 1999; Kaneko *et al.*, 1995; Peretz *et al.*, 2001). Transgenic mice expressing an anti-PrP mAb on B cells (Heppner *et al.*, 2001), immunization with recombinant PrP (Sigurdsson *et al.*, 2002) and passive immunization with an anti-PrP mAb (White *et al.*, 2003) antagonized the peripheral inoculation of scrapie-affected brain inoculum. These *in vivo* experiments suggested the possible use of anti-PrP antibodies as a therapy for prion diseases. However, it remains unclear how anti-PrP antibodies can antagonize PrP^{Sc} formation in cells. To address this point, in the current study, we evaluated a panel of anti-PrP mAbs against diverse epitopes for inhibition of PrP^{Sc} formation. We found that a mAb recognizing the octapeptide repeat sequence, a region that is not essential for PrP^{Sc} formation, reduced PrP^{Sc} accumulation in cells persistently infected with prions. Furthermore, our data suggest a possible link between cell-surface retention of PrP^{C} by anti-PrP antibodies and inhibition of PrP^{Sc} formation in cells.

METHODS

Antibodies and chemicals. The properties of anti-PrP mAbs used in this study have been described elsewhere (Kim *et al.*, 2004). The mAb against sarcomeric actin (clone alpha-Sr-1) was purchased from DAKO. Stock solutions of chlorpromazine, dextran sulfate 500 (DS500) and polyethyleneimine were prepared in deionized water, while E-64d was dissolved in DMSO and quinacrine in methanol. Culture medium containing each chemical compound or mAb was prepared freshly for each experiment.

Cell culture. The mouse neuroblastoma cell line Neuro2a (CCL-131; ATCC) was cultured in Dulbecco's modified Eagle's medium (ICN Biomedicals) with 10 % fetal bovine serum (FBS) and non-essential amino acids. Mouse neuroblastoma cells persistently infected with prions, originally established by Race *et al.* (1987), were cloned by limiting dilution. Subclone I3/I5-9, which possessed a high level of PrP^{Sc}, was used in this study. I3/I5-9 cells were maintained in Opti-MEM (Invitrogen) containing 10 % FBS and cells passaged fewer than 20 times were used for experiments.

Treatment of cells persistently infected with prions and sample preparation. Almost-confluent I3/I5-9 cells in 25 cm^2 flasks were split 1 : 20 into 35 mm tissue culture dishes. On day 2, the medium was replaced with 3 ml Opti-MEM containing 4 % FBS and each test compound or mAb, and the cells were cultured for a further 3 days. For PrP^{C} detection, the cells were washed with PBS and lysed with 300 µl lysis buffer A (1 % Zwittergent 3-14, 150 mM NaCl, 50 mM Tris/HCl, pH 7·5) supplemented with protease inhibitors (2 mM EDTA, 1 µg pepstatin ml^{-1}, 2 µg leupeptin ml^{-1}, 2 µM bestatin and 1 µg aprotinin ml^{-1}). After the removal of cell debris by low-speed centrifugation, samples were centrifuged at 45 000 r.p.m. for 30 min at 4 °C using the TLA 100.3 rotor of a Beckman Optima TLX and the resulting supernatants were used as a source of PrP^{C}. For the detection of PrP^{Sc}, cells were lysed with 300 µl lysis buffer B (5 mM EDTA, 0·5 % Triton X-100, 0·5 % sodium deoxycholate, 150 mM NaCl, 10 mM Tris/HCl, pH 7·5) and kept on ice for 30 min. Cell debris was removed by centrifugation for 5 min at 1000 r.p.m. A portion of the sample (10 %) was removed for determination of protein concentration using the DC protein assay (Bio-Rad) and the remaining portions were treated with 20 µg proteinase K ml^{-1} for 20 min at 37 °C. Proteolysis was terminated by the addition of 1 mM Pefabloc (Roche). The samples were then treated with DNase I (100 µg ml^{-1}) and RNase A (5 µg ml^{-1}) for 15 min at room temperature and centrifuged at 70 000 r.p.m. for 2 h at 4 °C using the TLA 100.3 rotor of a Beckman Optima TLX. The resulting pellets were dissolved in SDS-PAGE sample buffer.

SDS-PAGE and immunoblotting. SDS-PAGE was carried out using NuPAGE 12 % Bis-tris gels and MOPS-SDS running buffer according to the manufacturer's instructions (Invitrogen). After SDS-PAGE, proteins were transferred on to Immobilon-P PVDF membranes (Millipore) using a Transblot Mini Cell wet-type blotting apparatus (Bio-Rad) and NuPAGE transfer buffer (Invitrogen) at 60 V for 2 h. Immunoreactive proteins were detected using X-ray film as described elsewhere (Kim *et al.*, 2004). For quantitative analysis, immunoreactive proteins were visualized using the Western-Star Protein detection kit (TROPIX) according to the supplier's instructions and processed with an LAS-1000 lumino image analyser (Fujifilm). The intensity of the bands was quantified using Science Lab 98 Image Gauge software (Fujifilm).

Flow cytometric analysis. Adherent cells were treated with ice-cold PBS containing 0·1 % collagenase (Wako) and dispersed by pipetting. Cells were washed with 0·5 % FBS in PBS (FBS/PBS) and incubated with anti-PrP mAbs diluted with 0·5 % FBS/PBS for 30 min on ice. Cells were washed three times with 0·5 % FBS/PBS and incubated with 1 : 2000-diluted Alexa 488-labelled Fab fragment of goat anti-mouse IgG (Molecular Probes) for 30 min. After washing, cells were stained with 5 µg propidium iodide ml^{-1} in 0·5 % FBS/PBS for 5 min and analysed using an EPICS XL-ADC flow cytometer (Beckman Coulter). All procedures were carefully carried out under chilled conditions.

Indirect immunofluorescence assay. Cells grown in eight-well slides (Nunc) were fixed with 100 % methanol for 20 min at −20 °C. Fixed cells were blocked with 5 % FBS/PBS for 30 min at room temperature, after which they were incubated with hybridoma supernatants or mAbs diluted in 1 % FBS/PBS for 30 min at room temperature. After washing with PBS, cells were incubated with 1 : 1000-diluted Alexa 488-labelled Fab fragment of goat anti-mouse IgG for 30 min. Finally, the slides were mounted with PBS containing 50 % glycerol and 1 % n-propyl gallate (Wako) and examined using a fluorescence microscope equipped with a cooled CCD unit (*Cool*SNAP HQ; Roper).

Cell growth and cytotoxicity. The effect of mAbs on cell growth was analysed using the 4-[3-(4-iodophenyl)-2-(4-nitrophenyl)-2H-5-tetrazolio]-1,3-benzene disulfonate (WST-1) assay (Ishiyama *et al.*, 1996) and cytotoxicity was analysed by lactate dehydrogenase (LDH) release assay using the LDH-Cytotoxic Test (Wako).

RESULTS

Anti-PrP mAbs inhibit PrP^{Sc} accumulation in cultured cells

Several antibodies recognizing regions in the C-terminal portion of PrP have been reported to inhibit PrP^{Sc} accumulation in neuroblastoma cells persistently infected with prions (Enari *et al.*, 2001; Peretz *et al.*, 2001). We recently established a panel of diverse anti-PrP mAbs including those recognizing the octapeptide repeat in the N-terminal region of PrP (Kim *et al.*, 2004). In the current studies, we investigated whether they would effect PrP^{Sc} accumulation in prion-infected neuroblastoma cells. Fig. 1(a) shows the effect of mAbs recognizing linear epitopes on PrP^{Sc} accumulation in I3/I5-9 cells persistently infected with prions. Following a 3-day treatment, only two mAbs reduced PrP^{Sc} accumulation: 31C6, which recognizes aa 143–149 of mouse PrP, and 110, which recognizes PHGGGWG at aa 59–65 and aa 83–89 in the octapeptide repeat. Quantitative analysis revealed that other mAbs did not affect the total amount of PrP^{Sc}, or the ratio of di-, mono- and non-glycosylated PrP^{Sc}.

Flow cytometric analysis showed that mAbs 110 and 31C6 bound PrP^{C} on the cell surface, although the fluorescence intensity of mAb 110 was weaker than that of mAb 31C6 (Fig. 1b, left panel). In contrast, mAbs that had no effect on PrP^{Sc} accumulation did not appear to bind to PrP^{C} on the cell surface (Fig. 1b, right panel). Two other mAbs, 44B1 and 72, which are thought to recognize discontinuous epitopes (Kim *et al.*, 2004), reacted with PrP^{C} on the cell surface (Fig. 1b) and inhibited PrP^{Sc} accumulation (Fig. 2). These results suggested that mAbs that can bind to PrP^{C} on the cell surface have the potential to antagonize PrP^{Sc} accumulation in cells persistently infected with prions.

Fig. 2 shows the dose-dependence of the effect of the anti-PrP mAbs. The four effective mAbs (110, 31C6, 44B1 and 72) reduced the amount of PrP^{Sc} in a dose-dependent manner, although PrP^{Sc} was not completely eliminated following the 3-day treatment. The 50 % effective dose (EC_{50}) of mAbs 110, 31C6, 44B1 and 72 was estimated to be 0·2 μg ml^{-1}(1·2 nM), 0·1 μg ml^{-1} (0·7 nM), 0·3 μg ml^{-1} (1·7 nM) and 0·6 μg ml^{-1} (4·1 nM), respectively (Fig. 2b).

Fig. 3 shows the long-term effect of mAbs on PrP^{Sc} formation. Treatment for 6 days with mAb 110, 44B1, 31C6 (Fig. 3) or 72 (data not shown) reduced PrP^{Sc} to an almost undetectable level, and no re-emergence of PrP^{Sc} was observed in the following 6 and 12 days of incubation in the absence of mAbs. On the contrary, mAbs that did not bind to cell-surface PrP^{C} showed little effect on PrP^{Sc} accumulation even after long-term treatment.

The influence of mAbs on cell growth and acute toxicity was examined by WST-1 assay and LDH release assay, respectively. No significant effect on cell growth was observed, even with long-term treatment (5 μg ml^{-1} for 6 days) and mAbs did not demonstrate any acute toxicity (10 μg ml^{-1}) following 2 h of treatment.

Effect of anti-PrP mAbs on total amount of PrP^{C}

Fig. 1(a, lower panel) shows total PrP^{C} in the I3/I5-9 cells treated with mAbs for 3 days. The intensities of PrP^{C} bands were normalized with α-sarcomeric actin on the same blot and PrP^{C} levels relative to cells treated with negative control mAb (P1-284) are indicated at the bottom. Although there was a certain degree of variation, no marked difference was observed in the total amount of PrP^{C}. In contrast, after long-term treatment (6 days), the total amount of PrP^{C} in I3/I5-9 cells treated with mAb 110 or 44B1 appeared to be higher than that with the negative-control mAb or other anti-PrP mAbs (Fig. 3, top right panel). To confirm this further, we repeated the same experiment at least three times for the four inhibitory mAbs, 110, 31C6, 44B1 and 72. Relative PrP^{C} levels in cells treated with these four mAbs were 168 ± 38, 88 ± 23, 183 ± 54 and 103 ± 33 %, respectively. These results suggested that the effect of mAbs on PrP^{C} level varied depending on the mAb: mAbs 110 and 44B1 increased total PrP^{C} levels following long-term treatment, while mAbs 31C6 and 72 did not affect the total PrP^{C} level.

Cell-surface localization of the mAb–PrP^{C} complex

The N-terminal portion of PrP, including the octapeptide repeat, is not essential for PrP^{Sc} formation and/or prion propagation (Flechsig *et al.*, 2000; Rogers *et al.*, 1993). The finding that not only the mAbs recognizing the C-terminal part of PrP, such as 31C6 and 44B1, but also mAb 110 inhibited PrP^{Sc} accumulation in the neuroblastoma cells, together with the fact that only the mAbs that bound to cell-surface PrP^{C} showed an inhibitory effect, implied that the mAb–PrP^{C} interaction on the cell surface is essential for inhibition of PrP^{Sc} accumulation. To investigate this further, we analysed the dynamics of anti-PrP mAbs after their binding to the cell surface (Fig. 4). Neuro2a cells were treated with 10 μg mAb 31C6 ml^{-1} for 1 h, after which the cells were cultured for an additional 4 h without mAb. Cells were then harvested and stained with an Alexa 488-conjugated secondary antibody. As a control, cells cultured with mAb 31C6 for 1 h were immediately stained with the secondary antibody. Flow cytometric analysis showed no difference in fluorescence intensity between the two preparations, suggesting that the mAb–PrP^{C} complex remained on the cell surface, even after the additional 4 h culture in the absence of mAb. As I3/I5-9 cells are established by repeated limiting dilution, Neuro2a cells may not be a suitable uninfected control for I3/I5-9 cells. Hence, we carried out the same experiment using I3/I5-9 cells. It is known that elimination of PrP^{Sc} parallels the reduction of prion infectivity. Considering biosafety issues, we used I3/I5-9 cells cured of PrP^{Sc} by long-term treatment with mAb 44B1 for flow cytometric analysis. mAb 31C6 (Fig. 4) and

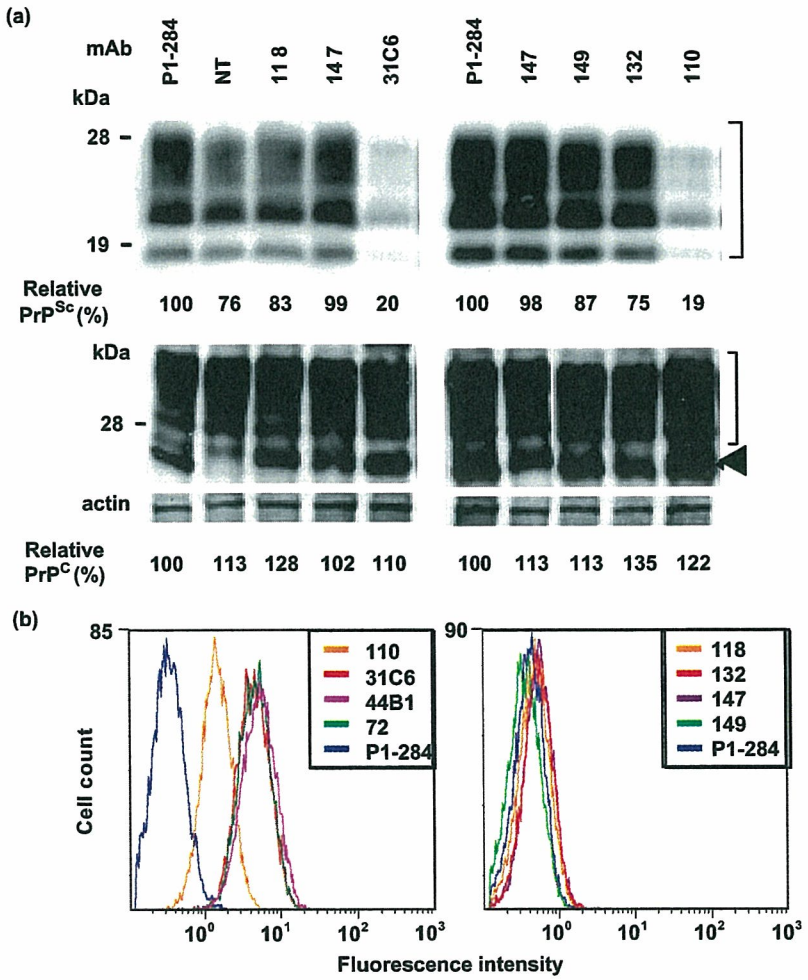

Fig. 1. Inhibition of PrP^{Sc} accumulation in prion-infected I3/I5-9 cells by anti-PrP mAbs. (a) Detection of PrP^{Sc} (upper panels) and PrP^{C} (lower panels). I3/I5-9 cells were cultured for 3 days with 4 % FBS in Opti-MEM containing 5 μg mAbs ml^{-1}. The level of PrP^{Sc} in the cells was determined by immunoblot analysis using mAb 44B1. Antibodies added to the culture are indicated above the panels. mAb P1-284 against feline panleukopenia virus was used as a control for non-specific effects. For detection of PrP^{Sc}, the load volume of each sample was adjusted based on the protein concentration of the corresponding cell lysate that had not been treated with proteinase K. For quantitative analysis of PrP^{Sc}, the three PrP^{Sc} bands indicated by a square bracket (right-hand side, upper panels) were grouped together. To check the ratios of the three PrP^{Sc} bands, each was selected separately. For PrP^{C}, the PrP^{C} bands indicated by a square bracket (right-hand side, lower panels) were quantified. The bands indicated by the arrowhead were excluded from the quantitative analysis, as they overlapped with immunoglobulin light chains that were detected by secondary antibodies. The blot used for PrP^{C} detection was also probed with anti-sarcomeric actin mAb for normalization. The levels of PrP^{Sc} and PrP^{C} relative to cells treated with negative-control mAb (P1-284) are indicated below the panels. NT, cells cultured without mAbs. Molecular mass markers are shown in kDa on the left. Epitopes for mAbs were as follows: 110, aa 56–89; 132, aa 119–127; 118, aa 137–143; 31C6, aa 143–149; 149, aa 147–151; 147, aa 219–229 (Kim *et al.*, 2004). (b) Binding of mAbs to the surface of Neuro2a cells examined by flow cytometry. The left panel shows mAbs that bound to the cell surface, while the right panel shows mAbs that did not bind. mAb P1-284 was used as a control for non-specific binding.

the three other inhibitory mAbs, 110, 44B1 and 72 (data not shown), showed the same retention of mAb–PrP^{C} complexes as observed with Neuro2a cells.

To confirm further the retention of mAb–PrP^{C} complexes on the cell surface, Neuro2a and I3/I5-9 cells were cultured for 1 h with mAbs 110, 31C6, 44B1 and 72, and, in some cases, the cells were cultured for an additional 4 h with mAb-free medium. The cells were then fixed with ice-cold methanol and mAb–PrP^{C} complexes were detected using secondary antibody (Fig. 5). All mAbs bound to the cell surface (Fig. 5a–e) and membrane staining could be detected, even after 4 h incubation in the absence of mAbs (Fig. 5f–j). To characterize further the retention of

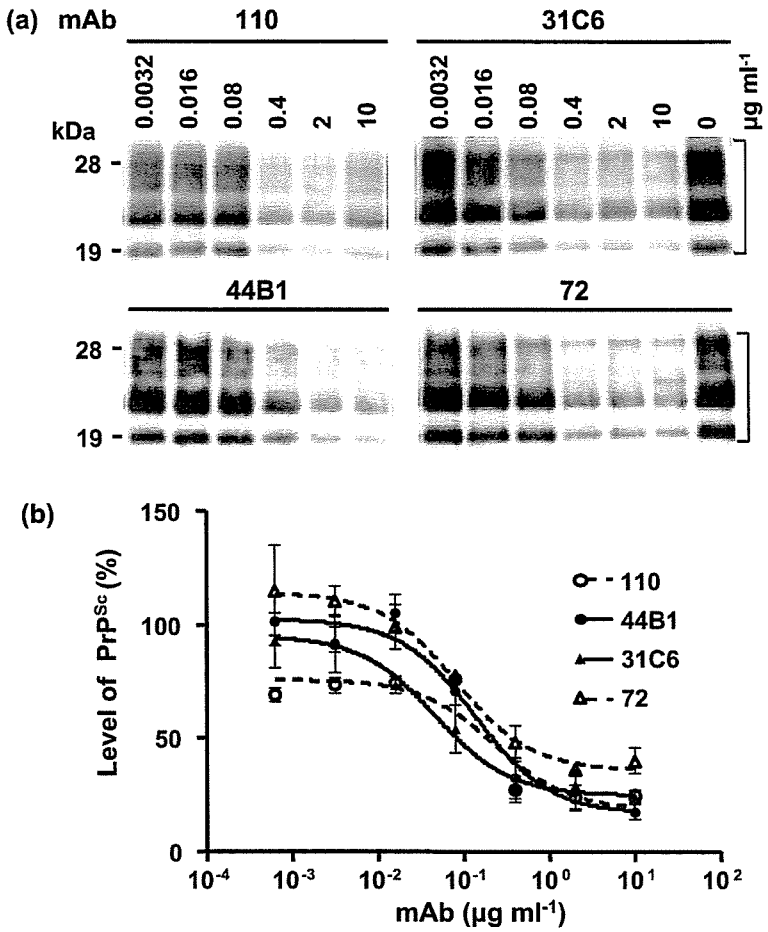

Fig. 2. Dose-dependent inhibition of PrP^{Sc} accumulation by anti-PrP mAbs. (a) Representative results from immunoblotting. I3/I5-9 cells were cultured for 3 days with various concentrations of mAb as indicated above the panels. The level of PrP^{Sc} was determined by immunoblot analysis using mAb 44B1. (b) Dose–response curve. The intensity of the PrP^{Sc} bands in the blots was quantified using an LAS-1000 lumino image analyser. The PrP^{Sc} level in the absence of mAbs was assigned a value of 100% in each experiment. The graph shows means ± SD from at least three independent experiments. EC_{50} values were estimated using GraphPad PRISM (GraphPad Software).

mAb–PrP^C complexes on the cell surface, we examined the effect of DS500, which is reported to accelerate PrP^C endocytosis (Shyng *et al.*, 1995). Following treatment with DS500, the mAb–PrP^C complexes on the cell surface were internalized and detected as intracellular granules (Fig. 5k–o). These results demonstrated that the mAbs bound to the cell-surface PrP^C remained there, regardless of their epitope specificity.

Effect of other compounds on PrP^C expression

Our results indicated a possible link between cell-surface retention of PrP^C by anti-PrP antibodies and the inhibition of PrP^{Sc} formation in cells, and suggested that the mAb treatment altered the total amount of PrP^C at least for mAbs 110 and 44B1. In order to examine whether compounds that inhibit PrP^{Sc} accumulation in prion-infected cells affect PrP^C level in the cells, we tested DS500, E-64d, quinacrine, chlorpromazine and polyethyleneimine. We confirmed that these compounds inhibited PrP^{Sc} accumulation in I3/I5-9 cells (data not shown). Using the concentrations at which these compounds caused >90% inhibition, we examined their effects on cellular levels of PrP^C following a 3-day treatment (Fig. 6a). Immunoblot analysis revealed that only DS500 reduced the PrP^C level (to ~30% that of untreated cells) among the compounds tested. Flow cytometric analysis with mAb 110 (Fig. 6b) confirmed that DS500 reduced the level of cell-surface PrP^C.

Since sulfated glycosaminoglycans like DS500 may bind to the N-terminal region of PrP^C (Pan *et al.*, 2002), the reduction in fluorescence intensity may be due to blocking of mAb 110 binding. For this reason, we used mAbs 31C6 and 44B1 to detect PrP^C instead of mAb 110. Table 1 shows the mean relative amount of PrP^C on the cell surface calculated from at least three independent experiments. Regardless of the mAb used for detection, DS500 reduced the PrP^C level to ~50% of the untreated control. No significant change in cell-surface expression of PrP^C was observed with the other compounds tested.

DISCUSSION

Anti-PrP antibodies that react with the C-terminal portion of PrP inhibit PrP^{Sc} formation in cultured cells (Enari *et al.*, 2001; Peretz *et al.*, 2001). One explanation for the inhibitory effect of these antibodies is that the binding of mAb to the corresponding epitope on PrP^C directly inhibits PrP^C–PrP^{Sc} interaction by occupying their binding domains. Fab D18, the most effective mAb reported by Peretz *et al.* (2001), reacts with the region spanning aa 132–156 in mouse PrP. In this study, we examined three mAbs

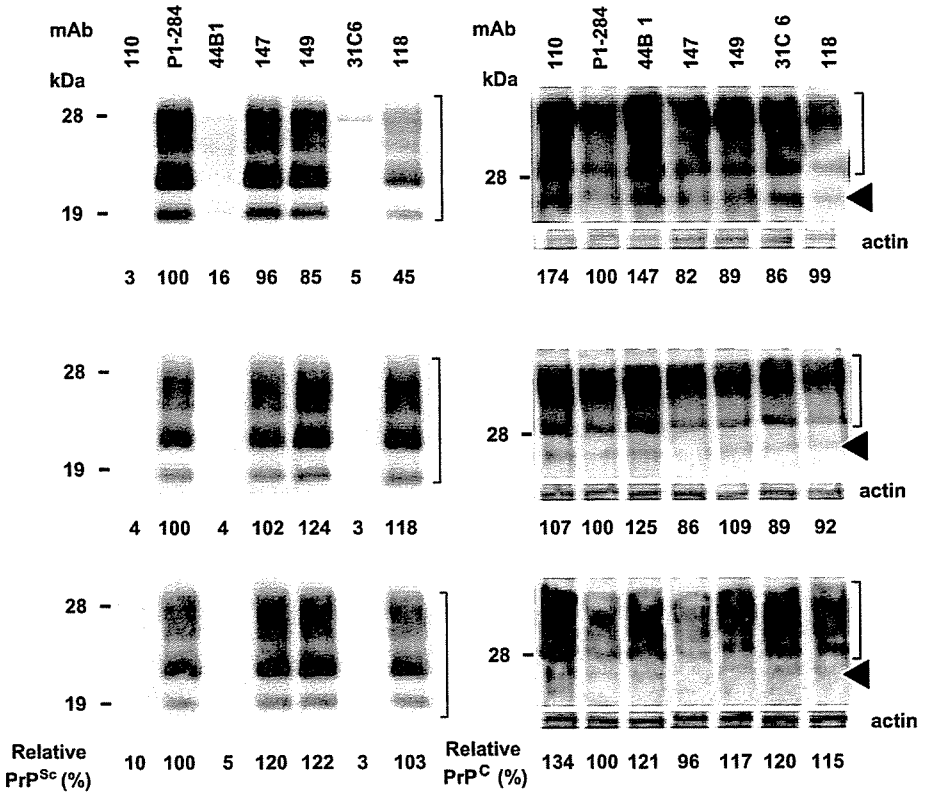

Fig. 3. Clearance of PrP^{Sc} by long-term antibody treatment. I3/I5-9 cells were cultured for 6 days with 5 μg mAb ml^{-1} (top panels). After withdrawal of the mAb, cells were cultured for an additional 6 (middle panels) or 12 (bottom panels) days in the absence of mAb. Quantitative analysis was carried out as described in the legend to Fig. 1 and relative PrP^{Sc} (left panels) and PrP^{C} (right panels) levels are indicated below the corresponding images.

recognizing epitopes within this region, but only mAb 31C6, which recognizes aa 143–149, displayed inhibitory activity. The remaining mAbs, 118 and 149, which bind adjacent epitopes aa 137–143 and aa 147–151, respectively, did not inhibit PrP^{Sc} formation in the cells. The main difference among these three mAbs was their ability to bind mature PrP^{C}; only mAb 31C6 bound PrP^{C} on the cell surface. Although it is well known that the N-terminal portion of PrP, including the octapeptide repeat, is not essential for prion propagation and/or PrP^{Sc} formation (Flechsig *et al.*, 2000; Rogers *et al.*, 1993), mAb 110, which recognizes the sequence in the octapeptide repeat, also antagonized PrP^{Sc} formation. This implied that there are mechanisms of inhibition other than blocking of the specific epitopes. Indeed, four of eight anti-PrP mAbs recognizing different epitopes inhibited PrP^{Sc} formation, suggesting that a common feature of the inhibitory mAbs is their ability to bind PrP^{C} on the cell surface. Taken together, our results suggest that inhibition of PrP^{Sc} formation by mAbs depends on their binding to mature PrP^{C} on the

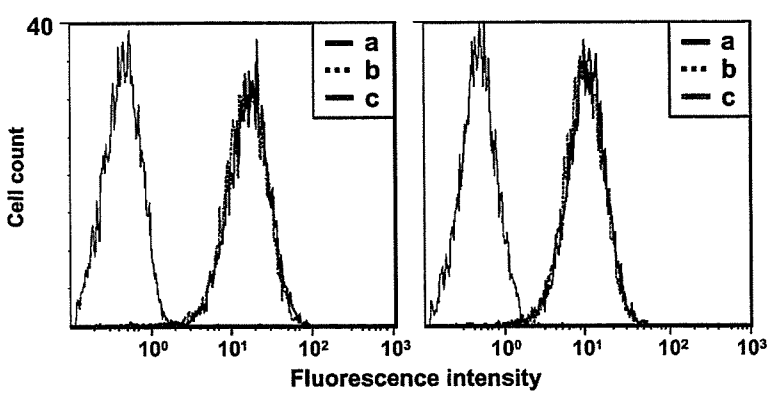

Fig. 4. Retention of mAb–PrP^{C} complexes on the cell surface. Neuro2a (left panel) or I3/I5-9 cells cured of PrP^{Sc} by mAb treatment (right panel) were cultured for 1 h in the presence of 10 μg negative control mAb P1-284 (a) or mAb 31C6 (b, c) ml^{-1}. Cells were harvested immediately and stained with Alexa-488-conjugated secondary antibody (a, b). Alternatively, after the removal of mAb, the cells were cultured for an additional 4 h in the absence of mAb and then harvested and stained with the secondary antibody (c).

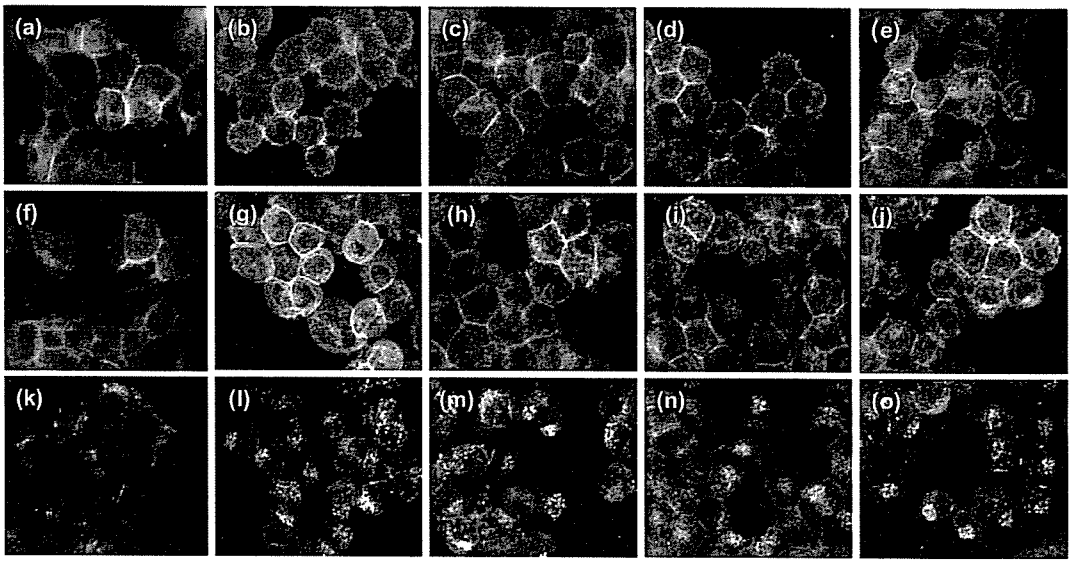

Fig. 5. Internalization of mAb–PrP^C complexes by treatment with DS500. Neuro2a cells (a, f and k) and I3/I5-9 cells (b–e, g–j, l–o) were cultured for 1 h with mAb 110 (b, g and l), 31C6 (a, f and k for Neuro2a cells; c, h and m for I3/I5-9 cells), 44B1 (d, i and n) or 72 (e, j and o). After removal of the mAb, cells were washed with ice-cold PBS and fixed with ice-cold methanol (a–e). Alternatively, after removal of mAb, cells were cultured with mAb-free medium for 4 h and fixed with ice-cold methanol (f–j). For DS500 treatment (k–o), after removal of mAb, cells were cultured for 3 h in mAb-free medium and then treated for 1 h with 25 μg DS500 ml^{-1}, after which they were fixed with ice-cold methanol. The fixed cells were directly stained with Alexa-488-conjugated secondary antibody to detect bound anti-PrP mAb.

cell surface rather than their binding to specific epitopes. On the other hand, transient interaction between the flexible N-terminal region and the second α-helix in the C-terminal globular domain has been postulated (Zahn *et al.*, 2000), and antibody binding to the N terminus of PrP prevents binding of C terminus-specific mAb (Li *et al.*, 2000). Hence, it cannot be excluded that binding of mAb 110 to the octapeptide repeat might sterically influence a particular domain involved in binding to PrP^{Sc}.

Although the cell-surface binding of mAb 110 was lower than that of the other mAbs (Fig. 1b, left panel), it inhibited PrP^{Sc} formation as efficiently. This may be explained by the presence of an 18 kDa N-terminally truncated PrP^C. This truncated PrP^C fragment is produced by cleavage of PrP^C around residue 112 during the recycling process (Chen *et al.*, 1995) so that it is not recognized by mAb 110. Recently, Mishra *et al.* (2002) reported that the N-terminally truncated form comprised as much as 40–50 % of PrP^C on the cell surface. This could account for the lower signals obtained using mAb 110. Because N-terminally truncated PrP^C is unlikely to act as a substrate for prion propagation and/or PrP^{Sc} formation (Lawson *et al.*, 2001; Weissmann, 1999), the binding of mAb 110 to PrP^C possessing the N-terminal portion is apparently sufficient for the inhibition of PrP^{Sc} formation.

In this work, we have demonstrated both quantitatively and qualitatively that mAbs that bind to cell-surface PrP^C remain attached to the membrane, even after withdrawal of the mAbs from the culture medium. This suggests that the mAb–PrP^C complex on the cell surface is not preferentially internalized into the cell. Mature PrP^C expressed on the cell surface is thought to be internalized via either clathrin-coated or -uncoated vesicles from which it enters the degradation pathway (Peters *et al.*, 2003; Shyng *et al.*, 1994; Sunyach *et al.*, 2003). Because PrP^{Sc} formation is believed to take place in the subcellular compartments that include cell membrane during the degradation pathway (Borchelt *et al.*, 1992; Caughey & Raymond, 1991), it is possible that mAb treatment could interfere with the regular PrP^C metabolism simply by retaining it on the cell surface. We suspected that the cell-surface retention of PrP^C would result in an increase in total PrP^C. Actually, two mAbs, 110 and 44B1, obviously increased the total amount of PrP^C, while two other mAbs 31C6 and 72 did not influence the total amount of PrP^C. It is conceivable that binding of mAbs to specific epitopes of cell-surface PrP^C might result in downregulation of PrP^C synthesis; however, further experiments are required to resolve this.

It was recently reported that polyclonal antibodies against dimeric recombinant PrP inhibited PrP^{Sc} formation in the cell, while the corresponding Fab fragments had little effect on PrP^{Sc} formation (Gilch *et al.*, 2003). This suggests that antibody-mediated cross-linking of PrP^C on the cell surface is important for inhibition of PrP^{Sc} formation. Whether cross-linking of PrP^C by IgG is required for the retention of the mAb–PrP^C complex under our experimental conditions remains to be determined. Treatment of cells persistently

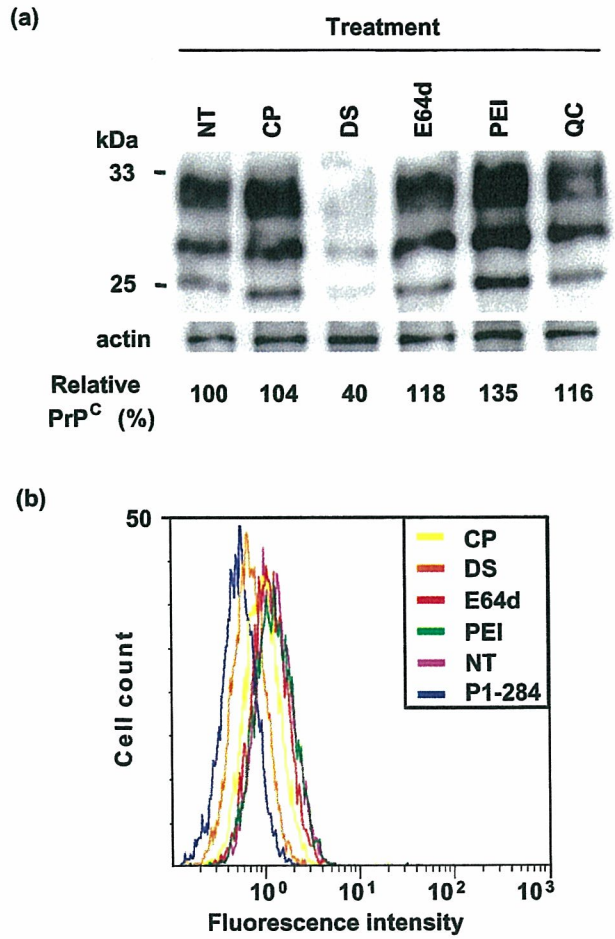

Fig. 6. Influence of chemical treatments on the expression of PrP^C. (a) Total amount of PrP^C. Neuro2a cells were treated for 12 h with various chemical compounds as indicated above the panel. Final concentrations were 3 μg chlorpromazine (CP) ml^{-1}, 25 μg DS500 (DS) ml^{-1}, 50 μM E-64d (E64d), 3 μg polyethyleneimine (PEI) ml^{-1} and 2 μM quinacrine (QC). Total PrP^C was detected in cell lysates by immunoblot analysis using mAb 31C6 (upper panel). The same blot was probed with anti-sarcomeric actin mAb to normalize for loading (lower panel). The intensity of the bands was quantified using an LAS-1000 lumino image analyser, and the relative amount of PrP^C compared with untreated control (NT) was calculated for each experiment. The data below the panel are means from three independent experiments. (b) Representative flow cytometric analysis of the cell-surface expression of PrP^C. Neuro2a cells were treated with compounds as described in (a), harvested, stained with mAb 110 followed by Alexa-488-conjugated secondary antibody and analysed by flow cytometry. The mean fluorescence intensity of the untreated control (NT) was assigned a value of 1 and the relative fluorescence intensities were calculated from the mean fluorescence intensity from each histogram. Quinarine was excluded from this experiment because of its autofluorescence. mAb P1-284 was used as a negative control for flow cytometric analysis.

Table 1. Effects of chemical treatment on cell-surface expression of PrP^C

Data represent means ± SD (minimum of $n=3$) of relative fluorescence intensity compared with control (NT).

Treatment	mAb for detection		
	110	31C6	44B1
NT	1·00	1·00	1·00
Chlorpromazine	0·77 ± 0·05	0·95 ± 0·03	0·92 ± 0·03
DS500	0·52 ± 0·03*	0·55 ± 0·10*	0·48 ± 0·04*
E-64d	0·99 ± 0·17	0·99 ± 0·06	0·97 ± 0·11
Polyethyleneimine	1·01 ± 0·16	1·04 ± 0·03	1·07 ± 0·11

*Statistically significant differences ($P<0·05$). The conditions of the treatments are described in the legend to Fig. 6.

infected with prions using antibodies against the laminin receptor precursor/laminin receptor (LRP/LR) reduced PrP^{Sc} accumulation (Leucht *et al.*, 2003). Because binding of LRP/LR to PrP^C could be involved in PrP metabolism (Gauczynski *et al.*, 2001), it is conceivable that antibodies interfere with the interaction between PrP^C and a molecule(s) that participates in PrP^C internalization.

Many reagents, including small molecules, recombinant PrP and anti-PrP antibodies, have been identified as potential inhibitors of prion propagation. It is important to elucidate their mechanisms of action, not only for the establishment of therapeutics but also for an understanding of prion replication. In the present study, we have demonstrated that blocking of the internalization of PrP^C with anti-PrP mAbs prevents PrP^{Sc} accumulation. Although anti-PrP mAbs recognizing specific epitopes have recently been reported to induce neuronal death in the hippocampus and cerebellum (Solforosi *et al.*, 2004), we have not found an apparent adverse effect on the cell growth and clinical manifestation by intraventricular inoculation of the anti-PrP mAbs used in this study (data not shown). Further analyses using prion-infected animals are necessary for evaluation of anti-PrP antibodies as therapeutics for treating prion diseases.

After the submission of this paper, a paper was published by Perrier *et al.* (2004) in which it was described that recognition by mAb SAF34 of the octapeptide repeat region on the N-terminal part of human PrP inhibited PrP^{Sc} formation in prion-infected neuroblastoma cells.

ACKNOWLEDGEMENTS

This work was supported by a grant from The 21st Century COE Program (A-1) and a Grant-in-Aid for Science Research (A) (grant 15208029) and (B) (grant 12460130) from the Ministry of Education, Culture, Sports, Science and Technology, Japan. This work was also supported by a grant from the Ministry of Health, Labour and Welfare of Japan.

REFERENCES

Borchelt, D. R., Taraboulos, A. & Prusiner, S. B. (1992). Evidence for synthesis of scrapie prion proteins in the endocytic pathway. *J Biol Chem* **267**, 16188–16199.

Bueler, H., Aguzzi, A., Sailer, A., Greiner, R. A., Autenried, P., Aguet, M. & Weissmann, C. (1993). Mice devoid of PrP are resistant to scrapie. *Cell* **73**, 1339–1347.

Caughey, B. & Race, R. E. (1992). Potent inhibition of scrapie-associated PrP accumulation by congo red. *J Neurochem* **59**, 768–771.

Caughey, B. & Raymond, G. J. (1991). The scrapie-associated form of PrP is made from a cell surface precursor that is both protease- and phospholipase-sensitive. *J Biol Chem* **266**, 18217–18223.

Caughey, B. & Raymond, G. J. (1993). Sulfated polyanion inhibition of scrapie-associated PrP accumulation in cultured cells. *J Virol* **67**, 643–650.

Caughey, W. S., Raymond, L. D., Horiuchi, M. & Caughey, B. (1998). Inhibition of protease-resistant prion protein formation by porphyrins and phthalocyanines. *Proc Natl Acad Sci U S A* **95**, 12117–12122.

Chabry, J., Caughey, B. & Chesebro, B. (1998). Specific inhibition of *in vitro* formation of protease-resistant prion protein by synthetic peptides. *J Biol Chem* **273**, 13203–13207.

Chen, S. G., Teplow, D. B., Parchi, P., Teller, J. K., Gambetti, P. & Autilio-Gambetti, L. (1995). Truncated forms of the human prion protein in normal brain and in prion diseases. *J Biol Chem* **270**, 19173–19180.

Demaimay, R., Adjou, K. T., Beringue, V., Demart, S., Lasmezas, C. I., Deslys, J. P., Seman, M. & Dormont, D. (1997). Late treatment with polyene antibiotics can prolong the survival time of scrapie-infected animals. *J Virol* **71**, 9685–9689.

Demaimay, R., Race, R. & Chesebro, B. (1999). Effectiveness of polyene antibiotics in treatment of transmissible spongiform encephalopathy in transgenic mice expressing Syrian hamster PrP only in neurons. *J Virol* **73**, 3511–3513.

Doh-Ura, K., Iwaki, T. & Caughey, B. (2000). Lysosomotropic agents and cysteine protease inhibitors inhibit scrapie-associated prion protein accumulation. *J Virol* **74**, 4894–4897.

Doh-ura, K., Ishikawa, K., Murakami-Kubo, I., Sasaki, K., Mohri, S., Race, R. & Iwaki, T. (2004). Treatment of transmissible spongiform encephalopathy by intraventricular drug infusion in animal models. *J Virol* **78**, 4999–5006.

Ehlers, B. & Diringer, H. (1984). Dextran sulphate 500 delays and prevents mouse scrapie by impairment of agent replication in spleen. *J Gen Virol* **65**, 1325–1330.

Enari, M., Flechsig, E. & Weissmann, C. (2001). Scrapie prion protein accumulation by scrapie-infected neuroblastoma cells abrogated by exposure to a prion protein antibody. *Proc Natl Acad Sci U S A* **98**, 9295–9299.

Flechsig, E., Shmerling, D., Hegyi, I., Raeber, A. J., Fischer, M., Cozzio, A., von Mering, C., Aguzzi, A. & Weissmann, C. (2000). Prion protein devoid of the octapeptide repeat region restores susceptibility to scrapie in PrP knockout mice. *Neuron* **27**, 399–408.

Gauczynski, S., Peyrin, J. M., Haik, S. & 8 other authors (2001). The 37-kDa/67-kDa laminin receptor acts as the cell-surface receptor for the cellular prion protein. *EMBO J* **20**, 5863–5875.

Gilch, S., Wopfner, F., Renner-Muller, I., Kremmer, E., Bauer, C., Wolf, E., Brem, G., Groschup, M. H. & Schatzl, H. M. (2003). Polyclonal anti-PrP auto-antibodies induced with dimeric PrP interfere efficiently with PrP^{Sc} propagation in prion-infected cells. *J Biol Chem* **278**, 18524–18531.

Heppner, F. L., Prinz, M. & Aguzzi, A. (2001). Pathogenesis of prion diseases: possible implications of microglial cells. *Prog Brain Res* **132**, 737–750.

Holscher, C., Delius, H. & Burkle, A. (1998). Overexpression of nonconvertible PrP^{c} Δ114–121 in scrapie-infected mouse neuroblastoma cells leads to *trans*-dominant inhibition of wild-type PrP^{Sc} accumulation. *J Virol* **72**, 1153–1159.

Horiuchi, M. & Caughey, B. (1999). Specific binding of normal prion protein to the scrapie form via a localized domain initiates its conversion to the protease-resistant state. *EMBO J* **18**, 3193–3203.

Horiuchi, M., Priola, S. A., Chabry, J. & Caughey, B. (2000). Interactions between heterologous forms of prion protein: binding, inhibition of conversion, and species barriers. *Proc Natl Acad Sci U S A* **97**, 5836–5841.

Ishiyama, M., Tominaga, H., Shiga, M., Sasamoto, K., Ohkura, Y. & Ueno, K. (1996). A combined assay of cell viability and *in vitro* cytotoxicity with a highly water-soluble tetrazolium salt, neutral red and crystal violet. *Biol Pharm Bull* **19**, 1518–1520.

Kaneko, K., Peretz, D., Pan, K. M. & 7 other authors (1995). Prion protein (PrP) synthetic peptides induce cellular PrP to acquire properties of the scrapie isoform. *Proc Natl Acad Sci U S A* **92**, 11160–11164.

Kaneko, K., Zulianello, L., Scott, M., Cooper, C. M., Wallace, A. C., James, T. L., Cohen, F. E. & Prusiner, S. B. (1997). Evidence for protein X binding to a discontinuous epitope on the cellular prion protein during scrapie prion propagation. *Proc Natl Acad Sci U S A* **94**, 10069–10074.

Kim, C.-L., Umetani, A., Matsui, T., Ishiguro, N., Shinagawa, M. & Horiuchi, M. (2004). Antigenic characterization of an abnormal isoform of prion protein using a new diverse panel of monoclonal antibodies. *Virology* **320**, 40–51.

Korth, C., May, B. C., Cohen, F. E. & Prusiner, S. B. (2001). Acridine and phenothiazine derivatives as pharmacotherapeutics for prion disease. *Proc Natl Acad Sci U S A* **98**, 9836–9841.

Ladogana, A., Casaccia, P., Ingrosso, L., Cibati, M., Salvatore, M., Xi, Y.-G., Masullo, C. & Pocchiari, M. (1992). Sulphate polyanions prolong the incubation period of scrapie-infected hamsters. *J Gen Virol* **73**, 661–665.

Lawson, V. A., Priola, S. A., Wehrly, K. & Chesebro, B. (2001). N-terminal truncation of prion protein affects both formation and conformation of abnormal protease-resistant prion protein generated *in vitro*. *J Biol Chem* **276**, 35265–35271.

Leucht, C., Simoneau, S., Rey, C., Vana, K., Rieger, R., Lasmezas, C. I. & Weiss, S. (2003). The 37 kDa/67 kDa laminin receptor is required for PrP^{Sc} propagation in scrapie-infected neuronal cells. *EMBO Rep* **4**, 290–295.

Li, R., Liu, T., Wong, B.-S. & 7 other authors (2000). Identification of an epitope in the C terminus of normal prion protein whose expression is modulated by binding events in the N terminus. *J Mol Biol* **301**, 567–573.

Mallucci, G., Dickinson, A., Linehan, J., Klohn, P. C., Brandner, S. & Collinge, J. (2003). Depleting neuronal PrP in prion infection prevents disease and reverses spongiosis. *Science* **302**, 871–874.

Mishra, R. S., Gu, Y., Bose, S., Verghese, S., Kalepu, S. & Singh, N. (2002). Cell surface accumulation of a truncated transmembrane prion protein in Gerstmann–Straussler–Scheinker disease P102L. *J Biol Chem* **277**, 24554–24561.

Murakami-Kubo, I., Doh-Ura, K., Ishikawa, K., Kawatake, S., Sasaki, K., Kira, J., Ohta, S. & Iwaki, T. (2004). Quinoline derivatives are therapeutic candidates for transmissible spongiform encephalopathies. *J Virol* **78**, 1281–1288.

Naslavsky, N., Stein, R., Yanai, A., Friedlander, G. & Taraboulos, A. (1997). Characterization of detergent-insoluble complexes containing the cellular prion protein and its scrapie isoform. *J Biol Chem* **272**, 6324–6331.

Pan, T., Wong, B. S., Liu, T., Li, R., Petersen, R. B. & Sy, M. S. (2002). Cell-surface prion protein interacts with glycosaminoglycans. *Biochem J* **368**, 81–90.

Peretz, D., Williamson, R. A., Kaneko, K. & 10 other authors (2001). Antibodies inhibit prion propagation and clear cell cultures of prion infectivity. *Nature* **412**, 739–743.

Perrier, V., Solassol, J., Crozet, C., Frobert, Y., Mourton-Gilles, C., Grassi, J. & Lehmann, S. (2004). Anti-PrP antibodies block PrP^{Sc} replication in prion-infected cell cultures by accelerating PrP^{C} degradation. *J Neurochem* **89**, 454–463.

Peters, P. J., Mironov, A., Jr, Peretz, D. & 8 other authors (2003). Trafficking of prion proteins through a caveolae-mediated endosomal pathway. *J Cell Biol* **162**, 703–717.

Priola, S. A., Raines, A. & Caughey, W. S. (2000). Porphyrin and phthalocyanine antiscrapie compounds. *Science* **287**, 1503–1506.

Race, R. E., Fadness, L. H. & Chesebro, B. (1987). Characterization of scrapie infection in mouse neuroblastoma cells. *J Gen Virol* **68**, 1391–1399.

Rogers, M., Yehiely, F., Scott, M. & Prusiner, S. B. (1993). Conversion of truncated and elongated prion proteins into the scrapie isoform in cultured cells. *Proc Natl Acad Sci U S A* **90**, 3182–3186.

Shyng, S. L., Heuser, J. E. & Harris, D. A. (1994). A glycolipid-anchored prion protein is endocytosed via clathrin-coated pits. *J Cell Biol* **125**, 1239–1250.

Shyng, S. L., Lehmann, S., Moulder, K. L. & Harris, D. A. (1995). Sulfated glycans stimulate endocytosis of the cellular isoform of the prion protein, PrP^{C}, in cultured cells. *J Biol Chem* **270**, 30221–30229.

Sigurdsson, E. M., Brown, D. R., Daniels, M., Kascsak, R. J., Kascsak, R., Carp, R., Meeker, H. C., Frangione, B. & Wisniewski, T. (2002). Immunization delays the onset of prion disease in mice. *Am J Pathol* **161**, 13–17.

Solforosi, L., Criado, J. R., McGavern, D. B. & 12 other authors (2004). Cross-linking cellular prion protein triggers neuronal apoptosis *in vivo*. *Science* **303**, 1514–1516.

Soto, C., Kascsak, R. J., Saborio, G. P. & 10 other authors (2000). Reversion of prion protein conformational changes by synthetic β-sheet breaker peptides. *Lancet* **355**, 192–197.

Sunyach, C., Jen, A., Deng, J., Fitzgerald, K. T., Frobert, Y., Grassi, J., McCaffrey, M. W. & Morris, R. (2003). The mechanism of internalization of glycosylphosphatidylinositol-anchored prion protein. *EMBO J* **22**, 3591–3601.

Supattapone, S., Nguyen, H.-O. B., Cohen, F. E., Prusiner, S. B. & Scott, M. R. (1999). Elimination of prions by branched polyamines and implications for therapeutics. *Proc Natl Acad Sci U S A* **96**, 14529–14534.

Supattapone, S., Wille, H., Uyechi, L., Safar, J., Tremblay, P., Szoka, F. C., Cohen, F. E., Prusiner, S. B. & Scott, M. R. (2001). Branched polyamines cure prion-infected neuroblastoma cells. *J Virol* **75**, 3453–3461.

Vey, M., Pilkuhn, S., Wille, H., Nixon, R., DeArmond, S. J., Smart, E. J., Anderson, R. G., Taraboulos, A. & Prusiner, S. B. (1996). Subcellular colocalization of the cellular and scrapie prion proteins in caveolae-like membranous domains. *Proc Natl Acad Sci U S A* **93**, 14945–14949.

Weissmann, C. (1999). Molecular genetics of transmissible spongiform encephalopathies. *J Biol Chem* **274**, 3–6.

White, A. R., Enever, P., Tayebi, M., Mushens, R., Linehan, J., Brandner, S., Anstee, D., Collinge, J. & Hawke, S. (2003). Monoclonal antibodies inhibit prion replication and delay the development of prion disease. *Nature* **422**, 80–83.

Xi, Y.-G., Ingrosso, L., Ladogana, A., Masullo, C. & Pocchiari, M. (1992). Amphotericin B treatment dissociates *in vivo* replication of the scrapie agent from PrP accumulation. *Nature* **356**, 598–601.

Zahn, R., Liu, A., Lührs, T. & 7 other authors (2000). NMR solution structure of the human prion protein. *Proc Natl Acad Sci U S A* **97**, 145–150.

NOTE *Clinical Pathology*

Unique Amino Acid Polymorphisms of PrP Genes in Mongolian Sheep Breeds

Altangerel GOMBOJAV[1,3], Naotaka ISHIGURO[1]*, Motohiro HORIUCHI[1] and Morikazu SHINAGAWA[2]

[1]*Laboratory of Veterinary Public Health, Obihiro University of Agriculture and Veterinary Medicine, Obihiro, Hokkaido 080–8555,*
[2]*Prion Disease Research Center, National Institute of Animal Health, 5–1–3 Kannondai, Tsukuba, Ibaraki 305–0856, Japan and*
[3]*School of Veterinary Medicine and Biotechnology, Mongolian State University of Agriculture, Ulaanbaatar 210153, Zaisan, Mongolia*

(Received 1 August 2003/Accepted 27 May 2004)

ABSTRACT. To characterize amino acid polymorphisms of sheep prion protein (PrP) gene, DNA from 740 sheep of nine breeds raised in Mongolia was isolated and analyzed. A total of 16 genotypes and seven allelic variants of the PrP gene at codons 112, 136, 154, and 171 were found. The MARQ/MARQ genotype associated with susceptibility to scrapie was found in 82.6% of the sheep while the MARR/MARR genotype associated with resistance to scrapie was found in 1.8% of the sheep. The polymorphisms of valine and serine at codon 127, and leucine and arginine at codon 189 were detected in eight Mongolian sheep breeds, suggesting that these polymorphisms are a common feature among Mongolian sheep breeds.
KEY WORDS: PrP genotype, scrapie susceptibility.

J. Vet. Med. Sci. 66(10): 1293–1295, 2004

Scrapie in sheep and goats is a fatal and infectious neurodegenerative disease that has been categorized as a transmissible spongiform encephalopathy (TSE) or prion disease also found in humans and other animals. Prion diseases are characterized by the accumulation in the tissues of the central nervous system of an "infectious" abnormal protease-resistant isoform (PrP^{Sc}) of cellular prion proteins (PrP^{C}) encoded by the PrP gene [12]. Polymorphisms of the PrP gene have been linked to host susceptibility and the incubation period of the disease [11]. PrP allelic variant valine/arginine/glutamine (VRQ) at codons 136, 154, and 171 is associated with high susceptibility to scrapie for sheep breeds. While the allele VRQ is rare in Suffolk sheep, the wild-type PrP allele alanine/arginine/glutamine (ARQ) is associated with susceptibility to scrapie. It has been widely considered that the PrP allelic variant alanine/arginine/arginine (ARR) at codons 136, 154, and 171 is associated with resistance to scrapie in several breeds [1–5, 7–10, 13]. Links between DNA polymorpisms and scrapie susceptibility have been identified in outbreaks of scrapie in various breeds or flocks in different countries where scrapie has been diagnosed [1, 7–8, 10, 13]. However, in central Asian countries where many sheep are raised, the polymorpism of PrP genes associated with scrapie have not yet been characterized. Therefore, we examined the PrP genotypes of 740 Mongolian sheep, including 271 sheep previously reported [6].

DNA samples were collected from several breeds from different prefectures in Mongolia. A total of 271 sheep came from the central region of Mongolia: 112 Khalkh sheep (native breed) from Tuv prefecture (designated I in Fig. 1.); 60 Khalkh sheep from Uvurkhangai prefecture (J); and 35 Yeroo sheep, 35 Orkhon sheep, and 29 Khangai sheep from Selenge prefecture (K) [6]. From the western region, a total of 345 sheep were used: 70 Khalkh sheep and 36 Sartuul sheep from Zavhan prefecture (A); 35 Khalkh sheep and 35 Govi-altai sheep from Govi-Altai prefecture (B); 71 Khalkh sheep and 33 Bayad sheep from Uvs prefecture (C); and 34 Khalkh sheep and 31 Darhad sheep from Huvsgul prefecture (D). For the eastern region, a total of 124 sheep were used: 32 Sumber Karakul sheep from Govi-Sumber prefecture (H); 32 Khalkh sheep from Dornogovi prefecture (E); 31 Khalkh sheep from Suhbaatar prefecture (F); and 29 Khalkh sheep from Hentii prefecture (G). The Khalkh sheep comprised about 90% of 13.8 million Mongolian sheep. Crossbreeding between the Khalkh sheep and local sheep including imported sheep started in the 1930s, and the crossbreeding has led to develop several local crossbreeds in Mongolia [6].

The entire 794-bp open reading frame (ORF) of the PrP gene was amplified by polymerase chain reaction (PCR) in 50 μl reactions, using PrP primers (SPrP-1, SPrP-2, SPrP-3, and SPrP-5) as described by Gombojav *et al.* [6]. To confirm amplification, a portion of each reaction product was electrophoresed on a 0.7% agarose gel containing ethidium bromide (0.5 $\mu g/ml$), and visualized under ultraviolet radiation. Then, the primers were removed using a Centricon 100 micro-concentrator (Amicon, Bedford, MA), and 1 to 5 μl of the concentrated PCR product was used for direct sequencing [6].

In this study, the relative genotype frequencies of four codons (112, 136, 154, and 171) of the PrP gene are newly reported in five sheep breeds (Sartuul, Govi-altai, Bayad, Darhad, and Sumber Karakul), in addition to four previously reported sheep breeds (Khalkh, Yeroo, Orkhon, and Khangai) [6]. Table 1 shows the genotype frequencies of 16 different PrP genotypes in the 740 sheep examined. The PrP genotypes MARQ/MARQ was found in all nine breeds.

Among all the breeds studied, the Khalkh sheep showed the greatest variation with 11 PrP genotypes composed from 6 alleles, while three to nine PrP genotypes were found in

* CORRESPONDENCE TO: ISHIGURO, N., Laboratory of Veterinary Public Health, Obihiro University of Agriculture and Veterinary Medicine, Obihiro, Hokkaido 080–8555, Japan.

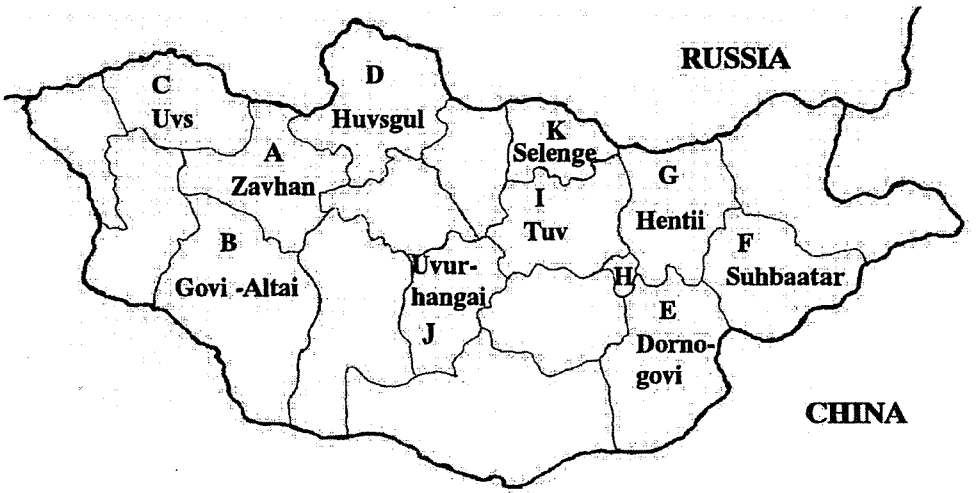

Fig. 1. Map of Mongolia. The blood samples were collected from different prefectures in Mongolia (A-K). H, Govi-Sumber prefecture.

Table 1. Frequency of PrP genotypes at codons 112, 136, 154 and 171 in Mongolian sheep breeds

Location[a]	A-G, I-J		A		B		C		D		H		K		K		K	
Breeds	Khalkh[b]		Sartuul		Govi-altai		Bayad		Darhad		Sumber		Yeroo[c]		Orkhon[c]		Khangai[c]	
PrP genotype	No	%	No	%	No	%	No	%	No	%	Karakul No	%	No	%	No	%	No	%
MARQ/MARQ	317	66.8	29	80.6	27	77.1	29	87.9	21	67.7	27	84.3	17	48.5	13	37.0	15	51.7
MARQ/TARQ	68	14.4	3	8.3	2	5.7	3	9.1	2	6.5			4	11.4	7	20.0	2	6.9
MARQ/MARH	31	6.6	2	5.5	2	5.7	1	3.0	5	16.2	3	9.4			1	2.9		
MARQ/MARR	13	2.7			2	5.7							8	22.8	8	22.8	9	31.0
MARH/MARH	7	1.5	1	2.8					1	3.2	2	6.3			1	2.9		
TARQ/TARQ	12	2.5							1	3.2			1	2.9				
TARQ/MARH	8	1.7													1	2.9		
TARQ/MARR	4	0.8			1	2.9									1	2.9		
MARQ/MAHQ	6	1.3																
MARR/MARR	7	1.5			1	2.9			1	3.2			2	5.7			2	6.9
MARK/MARK	1	0.2	1	2.8														
MARQ/MVRQ													1	2.9	2	5.7		
MARR/MVRQ													1	2.9				
MARH/MAHQ													1	2.9				
MARR/MAHQ															1	2.9		
TARQ/MAHQ																	1	3.5
Total	474		36		35		33		31		32		35		35		29	

a) Locations are shown in Fig. 1.
b) A total of 474 samples include 172 samples previously reported by Gombojav *et al.* [6].
c) Data from Gombojav *et al.* [6].

the other sheep breeds. The great variations in PrP genotypes suggest that Khalkh sheep originated from a mixture of several breeds from surrounding countries, while lesser variations in the other sheep breeds suggest that these breeds originated from a mixture of fewer numbers of breeds within Mongolia.

The allelic variant VRQ at codons 136, 154, and 171 is rare in Suffolk sheep [4, 9, 13] and this tendency was also found in the Mongolian sheep breeds. Valine at codon 136 (136V) associated with high susceptibility to scrapie was detected from two sheep breeds, Yeroo and Orkhon, but not in the other sheep breeds of Mongolia. Yeroo and Orkhon sheep have been raised in Selenge prefecture, which is in close proximity to Russia. The sheep raised in the prefecture had been genetically developed by crossbreeding with Russian sheep. Therefore, it is thought that the polymorphism of valine at codon 136 may have been introduced through the Russian sheep breeds, although little information about the PrP polymorphism of Russian sheep.

We found valine (V; nucleotides GTC) and serine (S;

Table 2. Frequency of PrP genotypes at codons 127 and 189 in Mongolian sheep breeds

Location[a]	A-G, I-J		A		B		C		D		H		K		K		K	
Breeds	Khalkh[b]		Sartuul		Govi-altai		Bayad		Darhad		Sumber		Yeroo[c]		Orkhon[c]		Khangai[c]	
PrP genotype	No	%	No	%	No	%	No	%	No	%	Karakul No	%	No	%	No	%	No	%
GQ/GQ[d]	354	74.6	26	72.2	17	48.6	22	66.8	20	64.5	23	71.9	28	80.0	32	91.4	29	100
GQ/SQ	68	14.4	5	13.9	4	11.4	6	18.2	8	25.8	5	15.6	7	20.0	1	2.9		
SQ/SQ	5	1.1									1	3.1						
GQ/VQ	19	4.0					1	3.0			2	6.3						
GQ/GL	20	4.2	4	11.1	11	31.4	2	6.0	3	9.7	1	3.1			2	5.7		
GL/GL	1	0.2																
GQ/GR	2	0.4			1	2.9												
GL/SQ	5	1.1	1	2.8	2	5.7	2	6.0										
Total	474		36		35		33		31		32		35		35		29	

a) Locations are shown in Fig. 1.
b) A total of 474 samples include 172 samples previously reported by Gombojav *et al.* [6]
c) Data from Gombojav *et al.* [6].
d) Wild type of sheep PrP gene.

AGC) at codon 127, and leucine (L; CTA) and arginine (R; CGA) at codon 189 in eight Mongolian sheep breeds (Table 2). These amino acid polymorphisms of PrP gene were widely observed in Mongolian sheep breeds but have not been reported in other sheep from European countries, suggesting that these are unique to indigenous sheep breeds including Mongolian sheep. However, it remains to be determined whether these polymorphisms have any correlation with susceptibility to scrapie.

Among the different sheep breeds raised in Mongolia, 66.9% had the MARQ/MARQ genotype and 1.8% had the MARR/MARR genotype, which are linked to susceptibility and resistance to scrapie, respectively (Table 1). In the previous study [6], we examined the scrapie form of the prion protein (PrP^{Sc}) in brain tissues from 10 sheep with neurological symptoms, but no PrP^{Sc} was obtained by Western blot analysis. Therefore, although there have been no reports of scrapie in Mongolia, these results suggest that the majority of Mongolian sheep are genetically susceptible to scrapie. However, since PrP genes linked to scrapie resistance were observed in five of the nine breeds, individual sheep carrying the scrapie-resistant genes can be identified and used in breeding programs to develop scrapie-resistant populations.

ACKNOWLEDGEMENTS. This work was partly supported by a grant from the Ministry of Health and Welfare of Japan, from Ministry of Agriculture, Forestry and Fisheries of Japan and Grant-in-Aid for Science Research from the Ministry of Education, Science and Culture of Japan (12460130, 12575030, 10556069).

REFERENCES

1. Belt, P.B.G.M., Muileman, I.H., Schreuder, B.E.C., Bos-de Ruijter, J., Gielkens, A.L.J. and Smits, M.A. 1995. *J. Gen. Virol.* **76**: 509–517.
2. Bossers, A., Screuder, B.E.C., Muileman, I.H., Belt, P.B.G.M. and Smits, M.A. 1996. *J. Gen. Virol.* **77**: 2669–2673.
3. Clouscard, C., Beaudry, P., Elsen, J.M., Milan, D., Dussaucy, M., Bounneau, C., Schelcher C.J., Launay, J.M. and Laplanche, J.L. 1995. *J. Gen. Virol.* **76**: 2097–2101.
4. Goldmann, W., Hunter, N., Foster, J.D., Salbaum, J.M., Beyreuther, K. and Hope, J. 1990. *Proc. Natl. Acad. Sci. U.S.A.* **87**: 2476–2480.
5. Goldmann, W., Hunter, N., Smith, G., Foster, J.D. and Hope, J. 1994. *J. Gen. Virol.* **75**: 989–995.
6. Gombojav, A., Ishiguro, N., Horiuchi, M., Serjmyadag, D., Byambaa, B. and Shinagawa, M. 2003. *J. Vet. Med. Sci.* **65**: 78–81.
7. Hunter, N., Foster, J.D., Goldmann, W., Stear, M.J., Hope, J. and Bostock, C. 1996. *Arch. Virol.* **141**: 809–824.
8. Hunter, N., Goldmann, W., Benson, G., Foster, J.D. and Hope, J. 1993. *J. Gen. Virol.* **74**: 1025–1031.
9. Hunter, N., Goldmann, W., Smith, G. and Hope, J. 1994. *Arch. Virol.* **137**: 171–177.
10. Laplanche, J.L., Chatelain, J., Westaway, D., Thomas, S., Dussaucy, M., Brugere-Picoux, J. and Launay, J.M. 1993. *Genomics* **15**: 30–37.
11. Loftus, B., Monks, E., Hanlon, J., Weavers, E. and Rogers, M. 1999. *Ir. Vet. J.* **52**: 81–85.
12. Prusiner, S.B. 1991. *Science* **252**: 1515–1522.
13. Westaway, D., Zuliani, V., Mirenda C.C., Da Costa, M., Neuman, S., Jenny, A.L., Detwiler, L. and Prusiner, S.B. 1994. *Genes. Dev.* **8**: 959–969.

Available online at www.sciencedirect.com
SCIENCE DIRECT®
Virology 320 (2004) 40–51
VIROLOGY
www.elsevier.com/locate/yviro

Antigenic characterization of an abnormal isoform of prion protein using a new diverse panel of monoclonal antibodies

Chan-Lan Kim,[a] Atsushi Umetani,[b] Toshio Matsui,[b] Naotaka Ishiguro,[a] Morikazu Shinagawa,[a,1] and Motohiro Horiuchi[a,c,*]

[a] *Laboratory of Veterinary Public Health, Obihiro University of Agriculture and Veterinary Medicine, Inada-cho, Obihiro, Hokkaido 080-8555, Japan*
[b] *Obihiro Research Laboratory, Fujirebio Inc., Kawanishi-cho, Obihiro, Hokkaido 089-1111, Japan*
[c] *Research Center for Protozoan Diseases, Obihiro University of Agriculture and Veterinary Medicine, Inada-cho, Obihiro, Hokkaido 080-8555, Japan*

Received 14 July 2003; returned to author for revision 22 October 2003; accepted 22 October 2003

Abstract

We established a panel of monoclonal antibodies (mAbs) against prion protein (PrP) by immunizing PrP gene-ablated mice with the pathogenic isoform of prion protein (PrP^{Sc}) or recombinant prion protein (rPrP). The mAbs could be divided into at least 10 groups by fine epitope analyses using mutant rPrPs and pepspot analysis. Seven linear epitopes, lying within residues 56–90, 119–127, 137–143, 143–149, 147–151, 163–169, and 219–229, were defined by seven groups of mAbs, although the remaining three groups of mAbs recognized discontinuous epitopes. We attempted to examine whether any of these epitopes are located on the accessible surface of PrP^{Sc}. However, no mAbs reacted with protease-treated PrP^{Sc} purified from scrapie-affected mice, even when PrP^{Sc} was dispersed into a detergent–lipid protein complex, to reduce the size of PrP^{Sc} aggregates. In contrast, denaturation of PrP^{Sc} by guanidine hydrochloride efficiently exposed all of the epitopes. This suggests that any epitope recognized by this panel of mAbs is buried within the PrP^{Sc} aggregates. Alternatively, if the corresponding region(s) are on the surface of PrP^{Sc}, the region(s) may be folded into conformations to which the mAbs cannot bind. The reactivity of a panel of mAb also showed that the state of PrP^{Sc} aggregation influenced the denaturation process, and the sensitivity to denaturation appeared to vary between epitopes. Our results demonstrate that this new panel of well-characterized mAbs will be valuable for studying the biochemistry and biophysics of PrP molecules as well as for the immunodiagnosis of prion diseases.

Keywords: Scrapie; Prion; BSE; Monoclonal antibody; Epitope mapping

Introduction

Transmissible spongiform encephalopathies (TSEs), so-called prion diseases, are fatal neurodegenerative diseases including scrapie in sheep and goats, bovine spongiform encephalopathy, and Creutzfeldt–Jakob disease (CJD) in humans (Prusiner, 1991). The causative agent, prion, is thought to be composed solely, if not entirely, of a pathogenic isoform of the prion protein (PrP^{Sc}). PrP^{Sc} is generated from a host-encoded cellular prion protein (PrP^{C}) by certain post-translational modifications including a conformational transformation. Although the two PrP isoforms share the same primary structure (Hope et al., 1986), PrP^{Sc} is distinguished from PrP^{C} by biochemical and biophysical properties such as high β-sheet content (Pan et al., 1993; Safar et al., 1993), partial resistance to protease digestion, and insolubility in nonionic detergent (Meyer et al., 1986). The conformational transformation from PrP^{C} to PrP^{Sc} requires preexisting PrP^{Sc} as a template and is thought to be a central event in PrP^{Sc} formation and prion replication. However, the molecular mechanism of the conformational transformation remains unclear. To elucidate the mechanism, structural information from two PrP isoforms is needed. At this time, the NMR structure of a recombinant PrP resembling PrP^{C} has been determined (Riek et al., 1996), whereas the structure of PrP^{Sc} is not yet known.

* Corresponding author. Laboratory of Prion Diseases, Graduate School of Veterinary Medicine, Hokkaido University, Kita 18, Nishi 9, Kita, Sapporo 060-0818, Japan. Fax: +81-11-706-5293.
E-mail address: horiuchi@vetmed.hokudai.ac.jp (M. Horiuchi).
[1] Present address: Prio Disease Research Center, National Institute of Animal Health, Kannondai, Tsukuba, Ibaragi, 305–0856, Japan.

0042-6822/$ - see front matter © 2004 Elsevier Inc. All rights reserved.
doi:10.1016/j.virol.2003.10.026

A diverse panel of anti-PrP mAbs is invaluable for analyzing the difference between PrP^{C} and PrP^{Sc}, as well as for the biochemical and structural analysis of PrP molecules. To date, many monoclonal antibodies (mAbs) against PrP have been generated by immunizing with PrP^{Sc} purified from scrapie-affected animals (Barry and Prusiner, 1986; Kascsak et al., 1987; Williamson et al., 1996), recombinant PrP (Zanusso et al., 1998), synthetic PrP peptides (Harmeyer et al., 1998; Horiuchi et al., 1995; O'Rourke et al., 1998), or a PrP expression plasmid (Krasemann et al., 1996). Most of the anti-PrP antibodies developed so far react with linear or discontinuous epitopes on PrP^{C} and recombinant PrP molecules, as well as with PrP^{Sc} treated with denaturant. These types of anti-PrP antibodies are now widely used for the immuno-detection of PrP^{Sc}. Because these antibodies themselves cannot distinguish the two PrP isoforms when the molecules are treated with denaturant, proteolytic removal of PrP^{C} before immuno-staining is essential for the detection of PrP^{Sc} by immunoblotting or enzyme-linked Immunosorbent assay (ELISA). One mAb, designated 15B3, generated by immunizing PrP gene-deficient mice with recombinant bovine PrP, was reported to recognize a PrP^{Sc}-specific conformational epitope consisting of two PrP molecules (Korth et al., 1997). However, further characterization of this mAb has not been published. Recent reports also describe mAbs that appear to recognize discontinuous epitopes on PrP^{C} but do not appear to react with PrP^{Sc} (Yokoyama et al., 2001).

Further PrP^{Sc}- and PrP^{C}-specific antibodies, as well as additional characterized antibodies to PrP molecules, will help to elucidate the structure–function relationships of PrP, structural differences between PrP^{C} and PrP^{Sc}, and mechanisms of conformational transformation. In addition, new antibodies showing higher reactivity and specificity than those currently available would help to improve the sensitivity of PrP^{Sc} detection. Although a large number of antibodies against PrP have been generated, it is possible that undefined epitopes still exist. In this study, we established a panel of mAbs that covers diverse epitopes on the mouse PrP molecules by immunizing $PrP^{-/-}$ mice with either recombinant mouse PrP or PrP^{Sc} purified from scrapie-affected mouse brains. The mAbs could be at least divided into 10 groups based on fine epitope mapping. Finally, we discuss how this panel of well-characterized mAbs will be useful for analyzing the molecular properties of PrP as well as for diagnostic purposes.

Results

Production of monoclonal antibodies against PrP molecules

For the immunization of PrP gene-ablated mice, we prepared rMoPrP as well as PrP^{Sc} from brains of scrapie-affected mice. Fig. 1 shows the purity of rMoPrP and PrP^{Sc}. rMoPrP23–231 expressed by pRSETB in *E. coli* formed inclusion bodies (Fig. 1A). The rMoPrP23–231 recovered from inclusion bodies was dissolved with 6 M GdnHCl, and further purified with Ni^{2+}-charged IMAC. After dialysis, rMoPrP possessing an intramolecular disulfide bond was

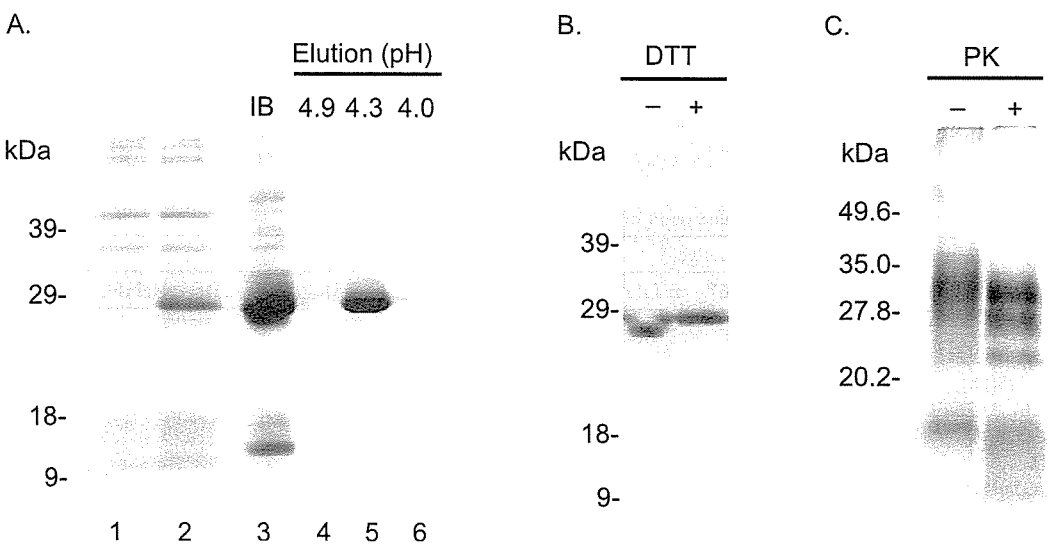

Fig. 1. Purity of rPrP and PrP^{Sc}. (A) Purification of rPrP from bacterial lysates. Whole lysates of *E. coli* transformed with pRSETB (lane 1) and pRSETB/MoPrP23–231 (lane 2) after induction with IPTG for 2 h. Inclusion bodies were prepared from whole bacterial lysates (lane 3) for partial purification of rPrP. Inclusion bodies were dissolved in 6 M GdnHCl and applied to Ni^{2+}-charged IMAC. The rPrP was eluted with a stepwise pH gradient (lanes 4–6), and rPrP eluted at pH 4.3 was dialyzed against acetate buffer to remove GdnHCl. (B) Formation of intramolecular disulfide bonds. After the dialysis, rPrP possessing an intramolecular disulfide bond was collected by reverse-phase HPLC. DTT + and – indicates purified rPrP dissolved with sample buffer with and without 100 mM DTT. (A and B) Coomassie blue staining. (C) Purity of PrP^{Sc} fraction from scrapie-affected mouse brains. The PrP^{Sc} fraction treated (+) and untreated (–) with PK was visualized by sliver staining and the purity was estimated by densitometric analysis by using Atto Densitograph (Atto Co. Ltd.). Molecular mass markers are in kilodaltons (kDa).

collected by reverse-phase HPLC (Fig. 1B). The $MoPrP^{Sc}$ prepared from brains of scrapie-affected mice was estimated to be >70% pure even without PK treatment (Fig. 1C), and a bioassay revealed that this fraction was estimated to contain more than10^{11} LD_{50}/mg from our dose–incubation time standard curve for Obihiro strain (data not shown). These PrP fractions were used for immunization of PrP gene-ablated mice, and splenocytes from immunized mice were fused with myeloma cells. Hybridomas positive for both rMoPrP and $MoPrP^{Sc}$, or those positive either for rMoPrP or $MoPrP^{Sc}$, were selected. Finally, we established 4, 10, and 15 hybridomas using rMoPrP23–231, rMoPrP89–231 or $MoPrP^{Sc}$, respectively, as the immunogen (Table 1).

Epitope analyses

To determine the epitopes recognized by the mAbs, we first examined their reactivity to various mutant rPrPs by ELISA. Based on their reactivity, the mAbs were divided into seven groups (Table 1). The mAbs in group I did not react with rMoPrP lacking the N-terminal region, indicating that their epitopes are located in residues 23–89. Group II mAbs reacted with all rMoPrPs except for rMoPrP155–231, indicating that they recognize the regions between residues 89 and 155. Group III consists of mAb 43C5, which reacted with all rMoPrPs, suggesting that its epitope is located between residues 155 and 167. The mAbs in group IV did not react with mutants lacking the C-terminus but reacted with other mutants, indicating that they recognize the epitopes on the C-terminal part of PrP molecule. The mAbs in group V reacted with rMoPrP155–231 but not with rMoPrP23–214. In addition, these mAbs did not react with point mutants rHaPrPC179A and rHaPrPC214A in which the cysteines at residues 179 and 214, respectively, were replaced with alanine. The mAbs reacted equally with rMoPrP23–231 and rHaPrP23–231 (data not shown), indicating amino acid differences between Mo and HaPrP did not influence the reactivity. These facts suggest that mAbs in groups V recognize discontinuous epitopes, including the region within residues 155–231, and that the epitopes are dependent on the intramolecular disulfide bond in the PrP molecule. The mAbs in group VI reacted with rMoPrP89–231, but neither reacted with rMoPrP155–231 nor point mutants of rHaPrP, suggesting that the epitope for these mAbs include the region within residues 89–231 and also are dependent on the intramolecular disulfide bond. The reactivity of mAb 72 (group VII) was difficult to figure out the epitope. It reacted with rMoPrP89–231 and 23–167, suggesting that the epitope is located within residues 89–167. However, the mAb did not react with rMoPrP23–214, rHaPrPC179A, or rHaPrPC214A, but reacted with rHaPrP23–231, again suggesting that the epitope depends on the presence of the intramolecular disulfide bond.

Further precise epitope mapping was carried out by pepspots analysis (Fig. 2). The reactivity of the group I mAbs revealed that they recognize a portion of octa-peptide repeat in N-terminus, although there is some difference in the amino acid sequence recognized by these mAbs. Based on the reactivity (Fig. 2A), the epitope for mAb 8 was WGQPHG at aa 56–61, 64–69, 72–77, and 80–85. mAbs 110 and 37 reacted with peptides 16–19 and 28–31, indicating that the recognized sequence is PHGGGWG at aa 59–65 and 83–89 (Fig. 2B). mAbs 40, 106, and 162 showed broad reactivity to peptides ranging from 13 to 33 (Fig. 2C). The reaction to peptides including 17 to 19 and 29 to 33 the most intense, suggesting that the major recognition sequence for these mAbs is PHGGGWGQ at aa 59–66 and 83–90, although the minimum required sequence appears to be WGQ. The group II mAb 132 reacted with peptides from 47 to 49, which share residues

Table 1
Grouping of mAbs based on the reactivity to rPrP deletion and point mutants

Group	mAb[a] (Isotype[b])	rPrP used as antigen[c]					
		rMoPrP23–167	rMoPrP23–214	rMoPrP89–231	rMoPrP155–231	rHaPrPC179A	rHaPrPC214A
I	8(2b), 37(2b), 40(2b), 106(2b), 110(2b), 162(2a)	+	+	–	–	+	+
II	13(2b), 32(2a), 118(2b), 132(G1), 149(2b), 31C6(G1)	+	+	+	–	+	+
III	43C5(G1)	+	+	+	+	+	+
IV	39(2b), 147(2b)	–	–	+	+	+	+
V	66(G1), 31B1(G1), 31B5(G1), 42B4(G1), 42D2(G1), 42D6(G1), 44A2(G1), 44A5(G1), 44B1(2a), 44B5(G1)	–	–	+	+	–	–
VI	23D9(G1), 42D3(G1), 44B2(G1)	–	–	+	–	–	–
VII	72(G1)	+	–	+	–	–	–

[a] MAbs named only with numbers were obtained by using $MoPrP^{Sc}$ as the immunogen, others named with a combination of numbers and letters were obtained using rMoPrP as the immunogen Among the latter, mAbs starting with 23 or 31, and 42, 43 or 44 were obtained by immunization with rMoPrP23–231 and rMoPrP89–231, respectively.
[b] G1, IgG1; 2a, IgG2a; 2b, IgG2b.
[c] Examined by ELISA.

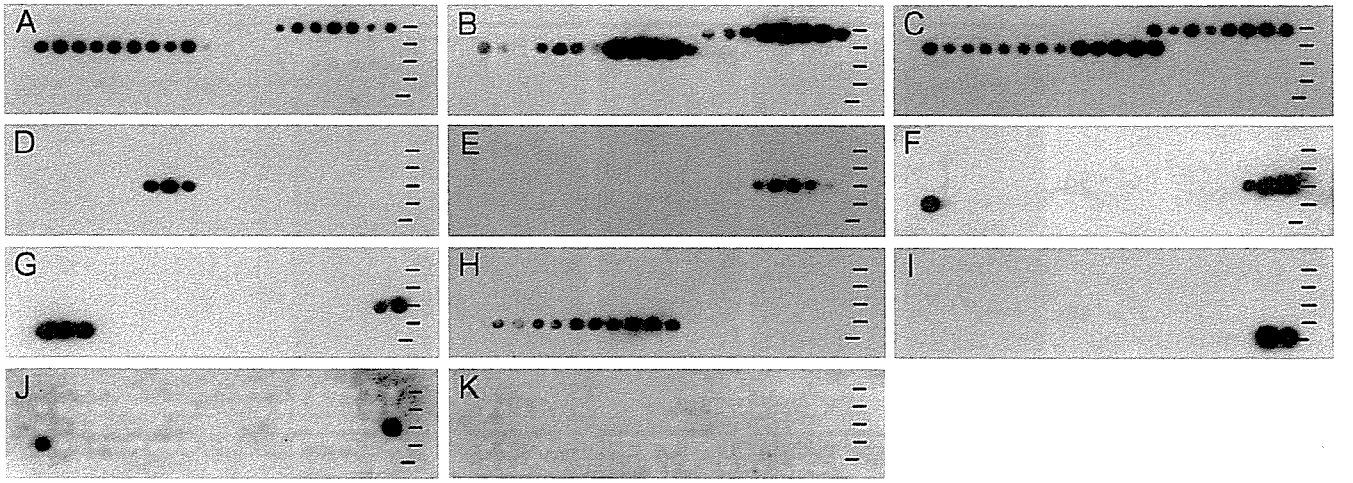

Fig. 2. Pepspot analysis. Bars on the right sides indicate lines of peptide spots. The first through fourth lines contain 20 spots per line, while fifth line contains 19 spots. (A) mAb 8 (group I); (B) mAb 110 (group I); (C) mAb 162 (group I); (D) mAb 132; (group IIa); (E) mAb 118 (group IIb); (F) mAb 31C6 (group IIc); (G) mAb 32 (group IId); (H) mAb 43C5 (group III); (I) mAb 147 (group IV); (J) mAb 72 (group VII); (K) mAb P1–284 (anti-parvovirus mAb, negative control).

119–127, AVVGGLGGY (Fig. 2D). mAbs 13 and 118 (group II) reacted with peptides from 55 to 58, which contain the fragment corresponding to residues 137–143, MIHFGND (Fig. 2E). The mAb 31C6 (group II) reacted with peptides from 58 to 61, which share in common residues 143–149, DWEDRYY (Fig. 2F). mAbs 32 and 149 (group II) reacted with five peptides from 59 to 63 that share a common sequence RYYRE, residues 147–151 (Fig. 2G). The mAb 43C5 (group III) reacted with 10 continuous spots but intense reactivity was observed to four peptides from 68 to 71, which contain the fragment corresponding to residues 163–169, RPVDQYS (Fig. 2H). This result is consistent with the epitope analysis of mutant recombinant PrPs. mAbs 39 and 147 (group IV) reacted with peptides 98 and 99, which correspond to the extreme C-terminus of PrP molecules, residues 219–229, KESQAYYDGRR (Fig. 2I). The mAbs in groups I–IV reacted with rHaPrPC179A and rHaPrPC214A in the ELISA (Table 1) and PrP^{Sc} in immunoblot analysis (Fig. 3), indicating that these mAbs recognize linear epitopes. mAb 72 appeared to recognize discontinuous epitope based on the reactivity to mutant rPrP (Table 1), although the mAb reacted with peptides 60 and 61, which share residues 143–153 (Fig. 2J).

Based on the fine epitope mapping by pepspot analysis, the mAbs in group II of Table 1 can be separated into four groups, designated IIa–IId. Together, the mAbs produced in this study can be divided into at least 10 groups; 7 that recognize linear epitopes, and 3 that recognize discontinuous epitopes (Table 2).

Species specificity of mAbs

We next examined the specificity of the mAbs by ELISA using species-specific versions of rMoPrP, rHaPrP, rShPrP, and rBoPrP. Most of the mAbs reacted with the rPrP from all four species (hamster, bovine, mouse and ovine), while the following mAbs showed obvious species-specific reactivity: mAbs 13 and 118 in group IIb, mAbs 39 and 147 in group IV, and mAb 66 reacted to Mo and HaPrP, while mAbs 42D2 and 44B5 showed intense reaction to Mo and HaPrP, moderate reaction to ShPrP but no reaction to BoPrP (data not shown).

Fig. 3 shows the reactivity to $MoPrP^{Sc}$, ovine PrP^{Sc} ($ShPrP^{Sc}$), and bovine PrP^{Sc} ($BoPrP^{Sc}$) in immunoblot analysis. mAbs 110, 132, 118, 31C6, 32, 43C5, and 147, which recognize linear epitopes, reacted with PrP^{Sc} prepared from brains of the disease-affected animals. Surprisingly, mAbs 44B1 and 72, which appeared to recognize discontinuous epitopes, showed an intense reaction to PrP^{Sc} in immunoblotting. The species-specific reactivities of mAbs 132, 118, 32, 43C5, 147, 44B1, and 72 are consistent with the results from ELISA; mAbs 118 and 147 only reacted with $MoPrP^{Sc}$ while other mAbs reacted with PrP^{Sc} from the other three species. In contrast to the results from ELISA, mAb 31C6 only reacted with $MoPrP^{Sc}$ and mAb 110 reacted with Mo and $ShPrP^{Sc}$ but not with $BoPrP^{Sc}$ in immunoblot analysis.

Reactivity of panel mAbs to purified PrP^{Sc}

To determine whether any of the antibody-reactive epitopes are exposed in the infectivity-associated PrP^{Sc}, we examined the reactivity of mAbs to purified $MoPrP^{Sc}$ by ELISA. A set of three PrP^{Sc} preparations, PK-untreated and non-denatured, PK-treated and non-denatured, and PK-treated and denatured, was used for each mAb (Fig. 4). All the mAbs reacted with PK-untreated non-denatured PrP^{Sc}, although the reactivity was lost when PrP^{Sc} was treated with PK. However, the mAbs regained reactivity when the PK-treated PrP^{Sc} was denatured with GdnHCl. These results suggest that the inability of the antibodies to react to PK-

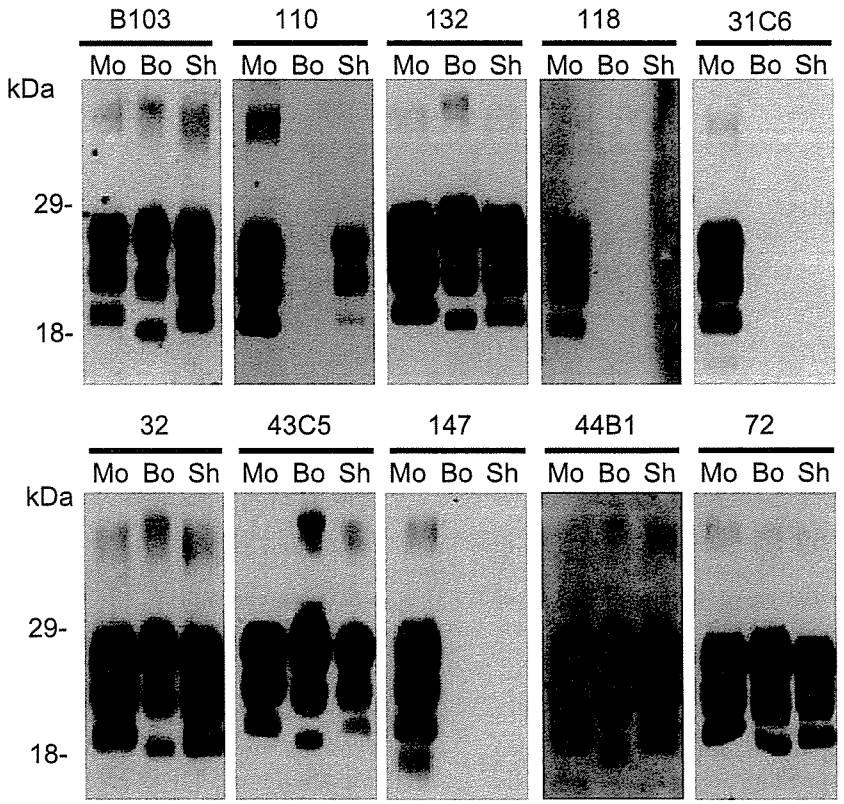

Fig. 3. Species specificity in Western blot analysis. Crude preparations of mouse (Mo), bovine (Bo), and sheep (Sh) PrP^{Sc} were prepared as described elsewhere (Grathwohl et al., 1997) and were separated by SDS-PAGE and transferred onto PVDF membranes. Brain tissue equivalents of 25 mg, 500, and 125 μg were loaded for Mo, Bo, and Sh PrP^{Sc}, respectively. The blots were stained with B-103 rabbit polyclonal antibodies (Horiuchi et al., 1995) or mAbs as indicated.

treated PrP^{Sc} is not due digestion of the PrP^{Sc}. Rather, it appears that the epitopes on PK-treated PrP^{Sc} are cryptic. A considerable amount of PK-sensitive PrP, including PrP^{C}, is co-purified during PrP^{Sc} purification in the absence of PK treatment (Caughey et al., 1995). Therefore, it is likely that reaction of the mAbs with PK-untreated non-denatured PrP^{Sc} accounts for the reaction to PK-sensitive PrP that exposes these epitopes on its accessible surface. Furthermore, the epitopes recognized by our panel of mAbs do not appear to be exposed on the surface of the PK-resistant core

Table 2
Characterization of mAbs against PrP

Group	mAb	Epitope[a]		Reactivity to PrP^{Sc} in ELISA[b]		
		position (amino acid)	L/DC	PK(−) GdnHCl(−)	PK(+) GdnHCl(−)	PK(+) GdnHCl(+)
I	8, 37, 40, 106, 110, 162	56–90	L	+	–	+
IIa	132	119–127	L	+	–	+
IIb	13, 118	137–143	L	+	–	+
IIc	31C6	143–149	L	+	–	+
IId	32, 149	147–151	L	+	–	+
III	43C5	163–169	L	+	–	+
IV	39, 147	219–229	L	+	–	+
V	66[c], 31B1, 31B5, 42B4, 42D2, 42D6, 44A2, 44A5, 44B1, 44B5[c]	155–231	DC	+(−)[c]	–	+(−)[c]
VI	23D9, 42D3, 44B2	89–231	DC	+	–	+
VII	72	89–231 (143–153)	DC	+	–	+

[a] L, linear epitope; DC, discontinuous epitope.
[b] Treatments of PrP^{Sc} are as described in Fig. 4.
[c] MAbs 66 and 44B5 reacted with rPrP but did not react with the three PrP^{Sc} preparations.

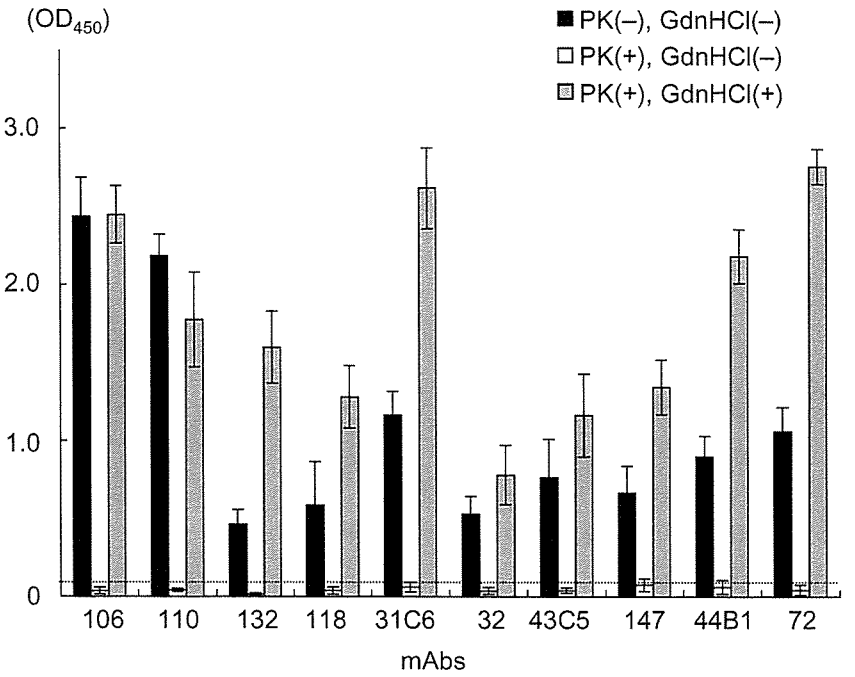

Fig. 4. Reactivity of mAbs to PrP^{Sc} fraction in ELISA. A set of three wells were used for each mAb: after the adsorption of purified PrP^{Sc} fraction, first well was neither treated with PK nor with GdnHCl [PK(–), GdnHCl(–)], second well was treated with 40 μg/ml PK for 60 min at 37 °C [PK(+), GdnHCl(–)], and third well was treated with PK and then further treated with 6M GdnHCl for 60 min to denature PrP^{Sc} [PK(+), GdnHCl(+)]. mAbs indicated in the figure were used as a representative for each group in Table 2. Dotted line indicates the cut-off value [An average OD_{450} value of negative control monoclonal antibody plus 5 times standard deviation ($n > 4$)].

of PrP^{Sc}. Instead, they become accessible to the mAbs after denaturation of PK-resistant core of PrP^{Sc}.

Reduction of PrP^{Sc} aggregate size does not expose cryptic epitopes

Purified PrP^{Sc} forms relatively large aggregates that can be precipitated by centrifugation at 10000 × *g*. We were concerned that the large aggregates themselves affect the antibody accessibility to PrP^{Sc}. To address this concern, we attempted detergent-lipid-protein complex (DLPC) treatment, which can reduce aggregate size without loss of infectivity (Gabizon et al., 1987). As shown in Fig. 5, nearly all of the purified PrP^{Sc} was present in the pellet after centrifugation at 10000 × *g* for 10 min, although more than the half of DLPC-treated PrP^{Sc} remained supernatant. Further centrifugation at 100000 × *g* of the soluble DLPC-treated PrP^{Sc} resulted in its precipitation. These results show that the DLPC treatment reduces the size of PrP^{Sc} aggregates without significant a loss of PK resistance. As described above (Fig. 4), mAbs did not react with PK-treated, DLPC-untreated PrP^{Sc} unless it was denatured (at 0 M GdnHCl in Fig. 6). Although all the mAbs except for mAbs 110, 132, and 32 faintly reacted with DLPC-treated PrP^{Sc} without denaturation (OD_{450} < 0.17 at 0 M GdnHCl), none of the mAbs showed a significant increase in reactivity to DLPC-treated PrP^{Sc} compared with DLPC-untreated PrP^{Sc}. These results suggest that the reduction of aggregate size by DLPC is not sufficient to expose cryptic epitopes on PrP^{Sc}.

Exposure of cryptic epitopes by denaturation

The reduction of PrP^{Sc} aggregate size by DLPC did not result in the efficient exposure of the hidden epitopes. In

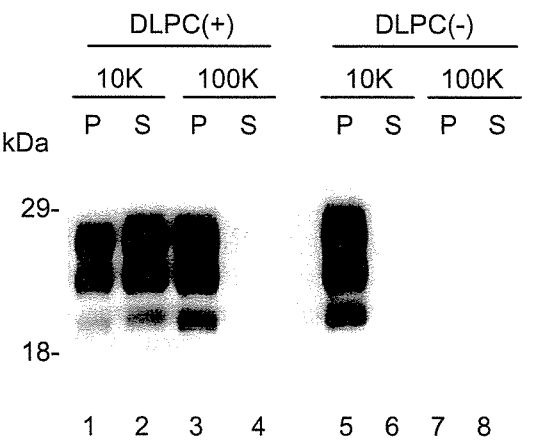

Fig. 5. Sedimentation analysis of DLPC-treated PrP^{Sc}. DLPC-treated (lanes 1–4) and untreated PrP^{Sc} (lanes 5–8) were digested by PK and then subjected to sedimentation analysis. Centrifugation at 10000 × *g* yielded pellet (lanes 1 and 5) and supernatant (lanes 2 and 6) fractions. The supernatants were further subjected to ultracentrifugation at 100000 × *g* to generate pellet (lanes 3 and 7) and supernatant (lanes 4 and 8). The PrP^{Sc} in each fraction was detected by immunoblot analysis.